AD-A045 858 DIKEWOOD INDUSTRIES INC ALBUQUERQUE N MEX F/G 20/3
THEORETICAL STUDY OF THE ELECTRICAL CORONA ON A LONG WIRE.(U)
APR 77 J LAM F29601-75-C-0120
UNCLASSIFIED DC-TN-1225-3 AFWL-TR-76-230 NL

1 OF 1
AD A045858



END
DATE FILMED
11-77
DDC

AFWL-TR-76-230

AD-A045858

THEORETICAL STUDY OF THE ELECTRICAL CORONA ON A LONG WIRE

Dikewood Industries, Inc.
Albuquerque, NM 87106

April 1977

Final Report

Approved for public release; distribution unlimited

AIR FORCE WEAPONS LABORATORY
Air Force Systems Command
Kirtland Air Force Base, NM 87117

DDC
RECEIVED
NOV 2 1977
D

AFWL-TR-76-230

This final report was prepared by the Dikewood Industries, Inc., Albuquerque, New Mexico, under Contract F29601-75-C-0120, Job Order 12090503 with the Air Force Weapons Laboratory, Kirtland Air Force Base, New Mexico. Mr W. D. Prather (ELPE) was the Laboratory Project Officer-in-Charge.

When US Government drawings, specifications, or other data are used for any purpose other than a definitiely related Government procurement operation, the Government thereby incurs no responsibility nor any obligation whatsoever, and the fact that the Government may have formulated, furnished, or in any way supplied the said drawings, specifications, or other data is not to be regarded by implication or otherwise as in any manner licensing the holder or any other person or corporation or conveying any rights or permission to manufacture, use, or sell any patented invention that may in any way be related thereto.

This report has been reviewed by the Office of Information (OI) and is releasable to the National Technical Information Service (NTIS). At NTIS, it will be available to the general public, including foreign nations.

William D Prather

WILLIAM D. PRATHER
Project Officer

FOR THE COMMANDER

Aaron B Loggins

AARON B. LOGGINS
Lt Colonel, USAF
Chief, Phenomenology & Technology Br

James L Griggs Jr

JAMES L. GRIGGS, JR.
Colonel, USAF
Chief, Electronics Division

DO NOT RETURN THIS COPY. RETAIN OR DESTROY.

UNCLASSIFIED

SECURITY CLASSIFICATION OF THIS PAGE (When Data Entered)

REPORT DOCUMENTATION PAGE		READ INSTRUCTIONS BEFORE COMPLETING FORM
1. REPORT NUMBER AFWL-TR-76-230	2. GOVT ACCESSION NO.	3. RECIPIENT'S CATALOG NUMBER
4. TITLE (and Subtitle) THEORETICAL STUDY OF THE ELECTRICAL CORONA ON A LONG WIRE		5. TYPE OF REPORT & PERIOD COVERED Final Report 6. PERFORMING ORG. REPORT NUMBER DC-TN-1225-3
7. AUTHOR(s) John Lam		8. CONTRACT OR GRANT NUMBER(s) F29601-75-C-0120
9. PERFORMING ORGANIZATION NAME AND ADDRESS Dikewood Industries, Inc. Albuquerque, New Mexico 87106		10. PROGRAM ELEMENT, PROJECT, TASK AREA & WORK UNIT NUMBERS 64747F 12090503
11. CONTROLLING OFFICE NAME AND ADDRESS Air Force Weapons Laboratory (ELPE) Kirtland Air Force Base, New Mexico 87117		12. REPORT DATE April 1977 13. NUMBER OF PAGES 56
14. MONITORING AGENCY NAME & ADDRESS(if different from Controlling Office)		15. SECURITY CLASS. (of this report) UNCLASSIFIED 15a. DECLASSIFICATION/DOWNGRADING SCHEDULE

16. DISTRIBUTION STATEMENT (of this Report)

Approved for public release; distribution unlimited.

17. DISTRIBUTION STATEMENT (of the abstract entered in Block 20, if different [illegible] report)

18. SUPPLEMENTARY NOTES

19. KEY WORDS (Continue on reverse side if necessary and identify by block number)

Electricity and Magnetism; Electromagnetic Fields and Waves; Corona; Discharge; Nonlinearities; Interaction and Coupling.

20. ABSTRACT (Continue on reverse side if necessary and identify by block number) (Unclassified Abstract)

This report contains a theoretical study of the electrical corona on a long wire. The physics of the phenomenon is discussed in detail, and formulated mathematically in terms of coupled nonlinear partial differential equations. A number of boundary-value problems for these equations are solved to predict the corona breakdown field and the d-c corona voltage-current characteristic. The results are in good agreement with experiment. Finally, the d-c corona effect on large signal propagation along a single wire above ground is examined by solving a

DD FORM 1 JAN 73 1473 EDITION OF 1 NOV 65 IS OBSOLETE

UNCLASSIFIED

SECURITY CLASSIFICATION OF THIS PAGE (When Data Entered)

nonlinear transmission line equation. The purpose of this study is to identify the set of basic corona equations as well as the mathematical nature of the problem. The application of these equations to analyze the corona effect on aircraft long-wire antennas will entail the solution of certain time-dependent problems of considerable mathematical complexity. These latter problems are not covered in the present study, and should form the subject of future investigations.

ACCESSION for
NTIS White Section X
DDC Buff Section ☐
UNANNOUNCED ☐
JUSTIFICATION.....
BY.....
DISTRIBUTION/AVAILABILITY CODES
Dist. AVAIL. and/or SPECIAL
A

PREFACE

Thanks are due to Phil Castillo, Bill Prather, and Denny Rossbach of the Air Force Weapons Laboratory for their unabated interest in the work, and to Gary Bedrosian, Kelvin Lee, and Lennart Marin at the Westwood Research Branch of the Dikewood Corporation for technical discussions and assistance.

CONTENTS

Section		Page
1	INTRODUCTION	1
2	PHYSICS OF THE CORONA	4
	2.1 Phenomenology	4
	2.2 Fundamental Processes in the Corona	6
	2.3 Mathematical Formulation	7
3	CALCULATION OF BREAKDOWN FIELD	12
	3.1 Quasi-Static Breakdown	12
	3.2 Microwave Breakdown	16
4	CALCULATION OF CORONA VOLTAGE-CURRENT CHARACTERISTIC	21
	4.1 Effect of Ion Mobility	21
	4.2 Effect of Ion Diffusion	24
	4.3 Effect of Ionization	31
5	APPLICATION TO A SINGLE LINE ABOVE GROUND	35
	5.1 Corona Voltage-Current Characteristic	35
	5.2 Corona Effect on Large Signal Propagation	41
6	CONCLUSIONS	50
	REFERENCES	52

ILLUSTRATIONS

Figure		Page
1	Coaxial electrode configuration for corona study.	13
2	Breakdown electric field E_c in air at normal temperature and pressure as a function of wire radius a. The crosses are data of Peek (ref. 1) taken at 60 Hz.	17
3	Normalized corona voltage-current characteristic for coaxial electrodes.	25
4	Comparison between theory and experiment for the d-c corona voltage-current characteristic according to Albrecht, Wagner and Bloss (ref. 11). Measurements were made for pure nitrogen at 1 atmosphere between coaxial electrodes with a = 0.5 mm., and b = 7 mm.	26
5	Normalized electric field $E(\rho)$, ion number density $n(\rho)$, and potential $V(\rho)$ across coaxial electrodes in corona with applied voltage difference $V = 2V_c$.	27
6	Wire-over-plane electrode configuration for corona study.	36
7	Bipolar coordinates.	38
8	Normalized corona voltage-current characteristic for wire-and-plane electrodes.	42
9	Semi-infinite transmission line over a ground plane.	43
10	Equivalent circuit for transmission line, with corona loss represented by nonlinear shunt conductance per unit length G(V).	45
11	Example of a double-exponential voltage pulse with peak value exceeding the corona onset voltage V_c.	48

SECTION 1

INTRODUCTION

On the surface of a good conductor the electric charges are highly concentrated in regions of small radii of curvature, such as tips, wires, edges and corners. As a consequence the local electric field can attain an enormous intensity. It can easily exceed a certain critical value beyond which ionization or breakdown of the surrounding air sets in. This critical or breakdown field strength is strongly dependent on atmospheric condition, and on conductor geometry and dimensions. At sea level its value is typically of the order of 30 kilovolts per centimeter, which is by no means altogether too high for common occurrence of the breakdown phenomenon. When ionization is initiated, the air becomes conducting and a discharging current flows through it from the conductor. The ionization and the discharge are accompanied by a visual display in the form of an eerie bluish or reddish glow crowning the high-field region. The discharge has thus acquired the name of a corona. When the corona appeared on top of the masts of a ship in a storm, it was often referred to by the ancient mariners as St. Elmo's fire. The corona is maintained until the discharge brings the local field strength down to below the critical value.

The corona discharge turns out to be an extraordinarily complex phenomenon in which scores of processes can participate. The net effect, however, is invariably the dissipation of electrical energy into heat, light, sound, and chemical energy. Not surprisingly, early study of the corona was carried out by the electrical power engineers. On a high-voltage power transmission line the surface electric intensity easily exceeds the corona onset value. The ensuing corona discharge constitutes a leakage current and a power loss. For a power line going over long distances the accumulative corona loss can be considerable. Out of this concern a number of investigators, notably Peek,[1] have conducted a series of detailed measurements on the corona properties, such as the breakdown field strength, the power loss, and the dependence on atmospheric and conductor conditions. The result is a set of empirical formulas directly applicable to power transmission calculations.

Another area of electrical engineering in which the corona discharge can exert considerable influence is the operation of large linear antennas. On Air Force aircraft, examples of such antennas are the LF/VLF trailing-wire antenna and the HF fixed-wire antenna. The transmitters can conceivably drive these antennas into the corona region, not to mention such intense electric field sources as lightning and the nuclear electromagnetic pulse. The appearance of coronas results in power dissipation, signal distortion and noise interference. Unfortunately there exist as yet few or no empirical formulas for a quantitative estimation of these effects, unlike in the case of power transmission engineering. This is due to the difficulty of making direct corona measurements on the antennas of a high-flying aircraft. On the other hand the high-altitude atmospheric environment and the free-flight aircraft-antenna configuration are not easy to simulate for measurement on the ground. It is desirable to conduct a theoretical study of the corona discharge from basic physical principles.

The corona discharge is a particular mode of the electric gas discharge which has been investigated extensively since the latter half of the 19th century. Out of this long-standing effort came the discovery of the electron, the invention of the X-ray and electron tubes, the development of quantum mechanics, and the complete theory of atomic structure. Today it can be safely claimed that gas discharge is no longer a mystery: no unknown fundamental mechanisms are believed to be at work behind the phenomenon. All participating physical processes are accounted for.[2] The general gas discharge theory can be formulated in terms of partial differential equations. Nevertheless, it is quite another matter to derive particular solutions of these equations describing particular modes of the discharge, such as the corona. As the equations are coupled and nonlinear, one has here the essential trappings of a very difficult mathematical problem.

This report studies various solutions of the basic gas discharge equations applicable to the corona on a long thin wire. Section 2 discusses the observational aspects of the electrical corona and the physical processes that take place in it. A set of basic equations are written down. Section 3 presents the solutions of two linear boundary-value problems of the basic equations to determine the corona breakdown field strengths for the coaxial cylindrical electrode geometry, both for quasi-static and for microwave

excitations. Section 4 solves three nonlinear boundary-value problems to calculate the post-breakdown d-c corona voltage-current characteristic for the coaxial electrode configuration, taking successively into account three major physical effects. Section 5 extends the d-c corona voltage-current characteristic calculations to the line-over-plane (or, equivalently, parallel-line) geometry. The results are applied to set up and solve nonlinear transmission line equations describing the d-c corona effect on signal propagation along a single line above a conducting ground plane. Finally, Section 6 discusses the limitations of the present results and the importance of some as yet unsolved problems.

It may be appropriate to state at the outset what these limitations and unsolved problems are. The present study forms the preliminary phase of an effort to determine the corona effect on aircraft long-wire antennas. Its goal is to establish the basic equations governing the general corona phenomenon, and to understand the mathematical nature of the antenna corona problem. A set of boundary-value problems of these basic equations are solved, and the solutions compare favorably with measurement. However, the results are valid only in the d-c or quasi-static regime. In the case of a long-wire antenna excited by an EMP or driven by an LF transmitter, the corona problem is, in general, a time-dependent boundary-value problem. The mathematical difficulty involved will be considerable. Its solution must be relegated to future investigations. More discussions on this point will be found below in Section 6.

SECTION 2

PHYSICS OF THE CORONA

2.1 Phenomenology

The electrical corona can be generated by the following apparatus arrangement in the laboratory. Take a long piece of thin well-polished wire and encase it in a large concentric cylindrical metallic shell. Apply a static voltage difference across the two conductors, with the wire positive. As the voltage is gradually raised and approaches a certain critical value, the electric field at the wire becomes very strong. Substantial ionization of the air molecules in the neighborhood takes place. When the critical threshold is exceeded, a luminous bluish uniform sheath appears on the wire surface, forming the corona proper. Its thickness grows with increasing applied voltage. The sheath is essentially a highly ionized plasma with positive and negative ions coexisting in comparable concentrations. The luminosity is a tell-tale sign of ion recombination and neutralization through the emission of photons. A shunt current can be detected to flow from the wire through the corona sheath and the dark space beyond into the outer cylinder. This indicates a dielectric breakdown of the air.

If now the experiment is repeated with the wire negative, the corona is observed to assume the form of isolated reddish tufts or beads more or less uniformly spaced along the wire. The breakdown voltage is also slightly off the positive corona value. The sign and size of the difference turn out to depend on gas, pressure and wire material. If the experiment is performed with an alternating voltage difference, the a-c corona appears only during that fraction of the period when the voltage exceeds the critical value. Its visual characteristics exhibit the same variation with wire polarity as for the d-c corona. Essentially the same corona observations can be made with the parallel-wire electrode arrangement. It must also be remarked that if the electrode spacing is very small, a spark discharge is observed and the corona is not formed.

Because of the possibility of substantial corona loss in high-voltage transmission, Peek[1] early this century made a series of careful measurements on long-wire corona characteristics. From the data he derived a set

of empirical formulas which are much respected even today. One set of formulas gives the breakdown electric field as a function of the wire radius; another set gives the corona loss as a function of the applied voltage. These are described below.

Breakdown Field. At normal temperature and pressure ($T \approx 25°C$, $p \approx 760$ mm. Hg) and an applied frequency of 60 Hz, the breakdown or critical electric field E_c on the wire surface of radius a at which the corona is initiated is given by

$$E_c = 31\left(1 + \frac{0.308}{\sqrt{a}}\right) \text{kV/cm.}, \qquad a \text{ in cm.} \tag{1}$$

for the coaxial geometry, and by

$$E_c = 29.8\left(1 + \frac{0.301}{\sqrt{a}}\right) \text{kV/cm.} \tag{2}$$

for the parallel-wire geometry. It is well to note that E_c depends only on the wire radius, irrespective of the location of the other electrode. For large a, E_c approaches a limit of about 30 kV/cm. which is often referred to as the dielectric strength of air. For small a, E_c diverges rapidly. The numerical constants in (1) and (2) vary with atmospheric condition. The quantitative dependence has been investigated by Peek, and more fully by Stephenson.[3]

Corona Loss. Peek measured the power loss due to corona and obtained the following empirical loss formula for a single line above ground:

$$P = 12(f+25)\sqrt{\frac{a}{2h}}\,(V-V_c)^2 \times 10^{-10} \text{ watts/meter} \tag{3}$$

where f is the applied frequency in hertz, a and h the wire radius and its height above ground, V and V_c are the peak values of the applied and critical voltages in volts relative to ground. V_c is related to the parallel-wire breakdown field in (2) by

$$V_c \approx aE_c \ell n\left(\frac{2h}{a}\right) . \tag{4}$$

Due to the difficulty in making precise high-voltage loss measurements, formula (3) is admittedly not very accurate, particularly for V close to V_c. The quadratic variation of P with the over-voltage is not always corroborated by the findings of other investigators. The noteworthy feature of (3) is the linear dependence of the loss on the applied frequency, indicating a constant loss per cycle.

2.2 Fundamental Processes in the Corona

The one basic physical process which underlies the corona phenomenon is the collision ionization of air molecules by free electrons. The latter are always present in air to some extent as a result of cosmic ray bombardment, natural radioactivity, air friction, and many other causes. In an intense electric field such as existing near a highly charged conductor, these mobile electrons are accelerated and quickly pick up sufficient energy to break up or ionize air molecules by collision, producing each time a positive ion and, what is important, one or more daughter electrons. These new electrons in turn can initiate collision ionizations on their own. When conditions are right, a chain reaction takes place. A large number of ions and electrons are produced in an instant, making the air conducting and able to sustain a discharge.

The criterion which permits the rapid build-up of charged particles in a small region of space is that the local rate of particle production by ionization exceed the rate of loss. The primary particle loss mechanisms are drift and diffusion. In an external electric field, charged particles drift along the field lines while suffering collisions with one another and with neutral particles. Diffusion arises from the microscopic random motion of these colliding particles, and is related to gas pressure. It forces particles to move from regions of high particle concentration to those of lower.

Besides the primary production and loss mechanisms of electron collisicn ionization, charged particle drift and diffusion, some secondary mechanisms are worth mentioning. Charged particles can also be produced by ion collision ionization, photo-ionization, and electrode emission.

They are also lost by electrode absorption, recombination (electrons and positive ions forming neutral molecules), and attachement (electrons attaching themselves to neutral molecules to form negative ions).

2.3 Mathematical Formulation

It remains to translate the above physical ideas into precise mathematical formulas. The most powerful analytical tool available to date for achieving this end is the Boltzmann transport equation, which describes the time development of a large aggregate of particles in terms of their fundamental microscopic interactions. This kinetic-theoretical approach will nevertheless not be adopted in the following calculations. A more coarse-grained formulation will be employed. It will be a continuum theory based on a set of hydrodynamic equations, which are the first few moment equations of the Boltzmann equation closed by truncation. These equations contain a number of transport coefficients which can either be calculated from first principles in kinetic theory or simply taken over from laboratory measurements.

The chief constituents of air are oxygen, nitrogen and hydrogen. The charged particles in air are therefore largely made up of their positive and negative ions and electrons. In the following an idealized model of ionized air will be used to make the calculations manageable. Ionized air will be taken to consist of one representative species of singly-charged positive ions and one representative species of singly-charged negative ions. They move under external and mutual forces over a background of neutral air molecules. This idealization is by no means an oversimplification, since experimentally it is often the averaged properties of ions of one sign that are directly measured. Essentially one deals here with a two-charged-fluid model of ionized air. The neutral molecules actually do not appear directly in the picture. The field variables are the particle number densities $n_{\pm}(\underline{r},t)$ of the two charged fluid components, and the total electric field $\underline{E}(\underline{r},t)$. The effect of magnetic fields on particle motion is negligible. The three variables are coupled together by three sets of field equations to be described below.

Equations of Motion. These equations express the particle current or flux densities $\underline{f}_{\pm}(\underline{r},t)$ in terms of the number densities $n_{\pm}$ and the

electric field $\underline{E}$. As mentioned previously, the motion of charged particles in air consists of a drift and a diffusion. The flux density has two corresponding components:

$$\underline{f} = \underline{f}_{\text{drift}} + \underline{f}_{\text{diffusion}} \tag{5}$$

The drift flux is given by

$$\underline{f}_{\text{drift}} = \pm K n \underline{E} \tag{6}$$

showing a direct proportionality of the drift velocity to the field. The physics behind this formula is that, in a weakly-ionized dense gas containing a large amount of neutral molecules, a charged particle moving in an electric field does not experience a sustained acceleration. As soon as enough kinetic energy is accumulated, it is lost through inelastic collisions with other particles. In fact, most energy is lost in ionizing *collisions with neutral molecules.* The effect of these collisions on the atomic level is the appearance of a macroscopic viscous force dragging the particle's movement. The drag soon counterbalances the electric field, and the particle henceforth moves on with a steady velocity proportional to the field. The constant of proportionality is the ion mobility K in Eq. (6). The mobility is always defined positive, so that a $\pm$ sign is needed in (6) to account for the oppositely directed motions of positive and negative charges in the field. Actually Eq. (6) is nothing but Ohm's law in disguise. This drag phenomenon has an analogue in parachute jump. After an initial gravitational acceleration, the viscous force of air soon equalizes gravity and the free fall proceeds at a uniform terminal velocity.

The diffusive flux density accounts for the random motion, due to random atomic collision, that is left out in (6). It is given by

$$\underline{f}_{\text{diffusion}} = -\nabla(Dn) \tag{7}$$

where D is the diffusion coefficient. In his investigation of Brownian motion, Einstein showed that, at thermal equilibrium,

$$\frac{D}{K} = \frac{k_B T}{e} \tag{8}$$

where e is the electronic charge, T the equilibrium temperature, and k_B the Boltzmann constant. The effect of diffusion is to even out particle densities, leveling off high concentrations and filling up depletions. In fact the phenomenon is mathematically equivalent to heat conduction.

In summary, the flux densities for positive and negative ions are

$$\underline{f}_+ = K_+ n_+ \underline{E} - \nabla(D_+ n_+) , \tag{9}$$

$$\underline{f}_- = -K_- n_- \underline{E} - \nabla(D_- n_-) . \tag{10}$$

Poisson's Equation. The total electric field consists of an external component due to the electrodes and an internal component due to the ions. It is determined by the Poisson equation:

$$\nabla \cdot \underline{E} = \frac{e}{\varepsilon_o} (n_+ - n_-) \tag{11}$$

with appropriate boundary conditions at the electrodes. The permittivity of air is taken to be essentially the same as that of free space.

Equations of Continuity. These equations express particle conservation. They balance out particle gain and loss mechanisms, and read

$$\frac{\partial n_+}{\partial t} + \nabla \cdot \underline{f}_+ = S(n_+, n_-, \underline{E}), \tag{12}$$

$$\frac{\partial n_-}{\partial t} + \nabla \cdot \underline{f}_- = S(n_+, n_-, \underline{E}). \tag{13}$$

where S is the net rate of particle production dependent on $n_\pm$ and $\underline{E}$. The right-hand sides of (12) and (13) are the same since positive and negative ions are produced or destroyed at the same rate in the same ionization or recombination processes. The functional form of S for electron collision ionization will be given below.

Equations (11), (12) and (13) form a set of coupled partial differential equations in $n_\pm$ and $\underline{E}$, with $\underline{f}_\pm$ defined by (9) and (10). The coefficients $\underline{D}_\pm$ and $K_\pm$ are usually regarded constant, with values taken from experiment.

These equations are nonlinear. The nonlinearities occur in the products $n_{\pm}\underline{E}$ and in S. Strictly speaking, the equations should be supplemented by another set describing energy conservation. As it turns out, corona energy dissipation proceeds mainly by way of ohmic loss[4] which is already implicit in Eq. (6).

Collision Ionization. When an electron moves through a gas under an electric field, the number of new electrons it produces by collision ionization along a unit length of its trajectory is experimentally found to be directly proportional to the local electron density:

$$dn_{-} = \alpha n_{-} d\ell \tag{14}$$

As is well-known, this type of relation produces exponential multiplication. The constant of proportionality α is known as Townsend's first ionization coefficient.[5] It is a nonlinear function of the local electric field, the nature of the gas, and the gas pressure. For a d-c field it is given to a good accuracy by the empirical formula:

$$\alpha = Ap \exp(-Bp/E) \tag{15}$$

where p is the gas pressure and A and B are empirical parameters. For air, the latter are found to be

$$A = 15 \text{ ion pairs/cm.} \times \text{mm. Hg} \tag{16}$$

$$B = 365 \text{ volts/cm.} \times \text{mm. Hg} \tag{17}$$

Then the ion production rate S due to collision ionization is given by

$$S = \alpha|\underline{f}_{-}| \tag{18}$$

In the following sections the above equations will be solved to study various aspects of the corona discharge from a long wire. It is to be noted that essentially the same set of equations occurs in the theory of

transistor p-n junction operation, the difference being in the relative magnitudes of the coefficients and parameters and in boundary conditions. The corona breakdown has a transistor analogue known as the avalanche breakdown of the p-n junction.

SECTION 3

CALCULATION OF BREAKDOWN FIELD

This section contains two calculations to determine the corona breakdown field in the quasi-static and microwave limits. The calculations involve the solution of two boundary-value problems for the ion equations (12) and (13). They will be carried out for the coaxial electrode configuration shown in Fig. 1. This highly symmetric geometry both simplifies the mathematics and makes possible comparison with measurements, as it is a favorite choice of the experimentalists.

This type of calculation is substantially simpler than the full-fledged corona problem. It deals mainly with the pre-breakdown regime when very few ions are formed. The electric field is not distorted by space charge, and nonlinearities do not occur. Consequently the Poisson equation is not needed. Furthermore, variations with time can be left aside if one is not concerned with the temporal development of the breakdown. The problem is mathematically one of determining the eigenvalues of linear ordinary differential equations.

3.1 Quasi-Static Breakdown

Suppose the wire in Fig. 1 is kept at a positive static potential V relative to the outer cylinder. Before breakdown there are very few ions in the intervening air, and the electric field is given by the familiar expression

$$\underline{E} = E\hat{e}_\rho, \qquad E(\rho) = E(a)\,\frac{a}{\rho}, \qquad E(a) = \frac{V}{a\ell n(b/a)}\,. \tag{19}$$

The ionization coefficient α in Eq. (15) becomes a function of space:

$$\alpha(\rho) = Ap\,\exp[-\frac{Bp}{aE(a)}\rho]. \tag{20}$$

Let a free electron be generated by some means at the surface of the outer electrode. It will travel radially inwards under the field, and on the way produce new electrons by ionizing collisions with air molecules. Upon reaching the inner wire it will have, according to (14), multiplied into an avalanche consisting

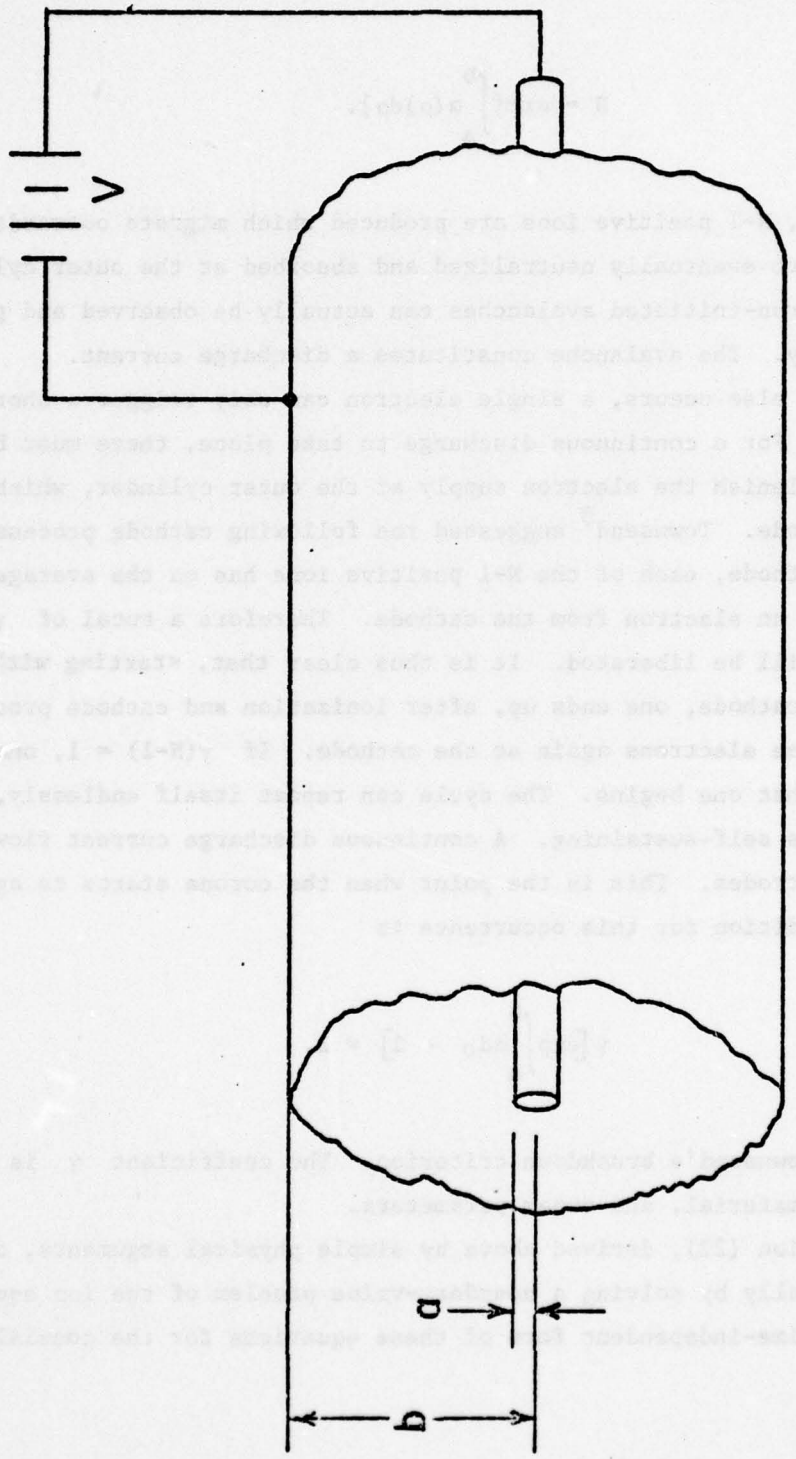


Figure 1. Coaxial electrode configuration for corona study.

of N electrons, with

$$N = \exp\left[\int_a^b \alpha(\rho)d\rho\right]. \tag{21}$$

At the same time, N-1 positive ions are produced which migrate outwards under the field, and are eventually neutralized and absorbed at the outer cylinder. Individual electron-initiated avalanches can actually be observed and photographed in the laboratory. The avalanche constitutes a discharge current.

If nothing else occurs, a single electron can only trigger a short discharge pulse this way. For a continuous discharge to take place, there must be some mechanism to replenish the electron supply at the outer cylinder, which in this case is the cathode. Townsend[5] suggested the following cathode process: upon impact on the cathode, each of the N-1 positive ions has on the average a probability γ of liberating an electron from the cathode. Therefore a total of $\gamma(N-1)$ free electrons will be liberated. It is thus clear that, starting with one free electron at the cathode, one ends up, after ionization and cathode processes, with $\gamma(N-1)$ free electrons again at the cathode. If $\gamma(N-1) = 1$, one ends up precisely with what one begins. The cycle can repeat itself endlessly, and the discharge becomes self-sustaining. A continuous discharge current flows between the electrodes. This is the point when the corona starts to appear. By (21), the condition for this occurrence is

$$\gamma\left[\exp\int_a^b \alpha d\rho - 1\right] = 1. \tag{22}$$

It is known as Townsend's breakdown criterion. The coefficient γ is dependent on gas, cathode material, and other parameters.

The condition (22), derived above by simple physical arguments, can also be obtained formally by solving a boundary-value problem of the ion equations (12) and (13). The time-independent form of these equations for the coaxial geometry is

$$\frac{1}{\rho}\frac{d}{d\rho}\left[\rho f_+(\rho)\right] = \alpha(\rho)\left|f_-(\rho)\right|, \tag{23}$$

$$\frac{1}{\rho}\frac{d}{d\rho}\left[\rho f_-(\rho)\right] = \alpha(\rho)\left|f_-(\rho)\right|. \tag{24}$$

It is convenient to introduce the total positive and negative ion fluxes $F_\pm(\rho)$ per unit length of wire such that

$$f_+(\rho) = \frac{F_+(\rho)}{2\pi\rho}, \qquad f_-(\rho) = -\frac{F_-(\rho)}{2\pi\rho}, \qquad F_\pm(\rho) \geq 0. \tag{25}$$

Then (23) and (24) become

$$\frac{d}{d\rho}F_+(\rho) = \alpha F_-(\rho), \qquad -\frac{d}{d\rho}F_-(\rho) = \alpha F_-(\rho). \tag{26}$$

The solution is

$$F_-(\rho) = F_-(b)\exp\left[\int_\rho^b \alpha d\rho\right], \tag{27}$$

$$F_+(\rho) + F_-(\rho) = \text{constant}. \tag{28}$$

The constants of integration are determined by boundary conditions at the electrodes. At the cathode $\rho = b$, one has $\gamma F_+(b) = F_-(b)$ as discussed above. At the anode $\rho = a$, namely the wire, the positive ion flux must be 0 since these ions are generated in air and migrate towards the cathode. Hence one has $F_+(a) = 0$. Substitution of (27) and (28) into the boundary conditions yields the following pair of homogeneous linear algebraic equations:

$$F_-(a) = F_-(b)\exp\left[\int_a^b \alpha d\rho\right], \tag{29}$$

$$\left(1 + \frac{1}{\gamma}\right)F_-(b) = F_-(a). \tag{30}$$

These equations have the trivial solution (namely zero ion current) unless the determinant vanishes. This condition is easily seen to be identical to (22). In other words, the solution describing the breakdown of the air gap between the electrodes is the eigen-solution of Eqs. (23) and (24).

At breakdown the field at the wire $E(a)$ is by definition the breakdown field E_c. Substitution of (20) into (22) yields

$$aE_c \frac{A}{B}\left[\exp\left(-\frac{Bp}{aE_c}a\right) - \exp\left(-\frac{Bp}{aE_c}b\right)\right] = \ln\left(\frac{1+\gamma}{\gamma}\right). \tag{31}$$

This relates E_c to the geometric, atmospheric, and other parameters of the problem. The solution showing the variation of E_c with a is plotted in Fig. 2 for A and B given by (16) and (17), $p = 760$ mm.Hg, $\gamma = 0.025$ for a copper cathode in air[6], and $b/a = 100$ as a typical radii ratio for the electrodes. Actually the result is totally insensitive to this last ratio, as the second exponential in (31) is entirely negligible for b only a few times larger than a. The breakdown data of Peek taken for concentric copper cylinders at 60 Hz[7] are also plotted for comparison. The data points follow the theoretical curve closely, making the same dramatic upturn for $a < 0.2$ cm. The measured values are about 10% lower than predicted. In view of the crudeness of the theory, which accounts only for ionization and cathode processes, the agreement between experiment and theory can be considered satisfactory. Much better agreement can certainly be achieved by adjusting the parameters in (31) to fit the data.

The above calculations are performed for a positive wire. It can be shown that exactly the same breakdown criterion is obtained for a negative wire. This theory therefore cannot account for the small dependence of the breakdown field on wire polarity.

3.2 Microwave Breakdown

In an applied electric field at microwave frequency, an ion moves quite differently than in a d-c field. The field reverses its direction every half-cycle, and the ion's motion is predominantly oscillatory. There is very little drifting motion, the mobility being inversely proportional to the applied frequency. In this limit the equation of continuity (13) for electrons becomes

$$\frac{\partial n_-}{\partial t} - \nabla^2(D_- n_-) = S. \tag{32}$$

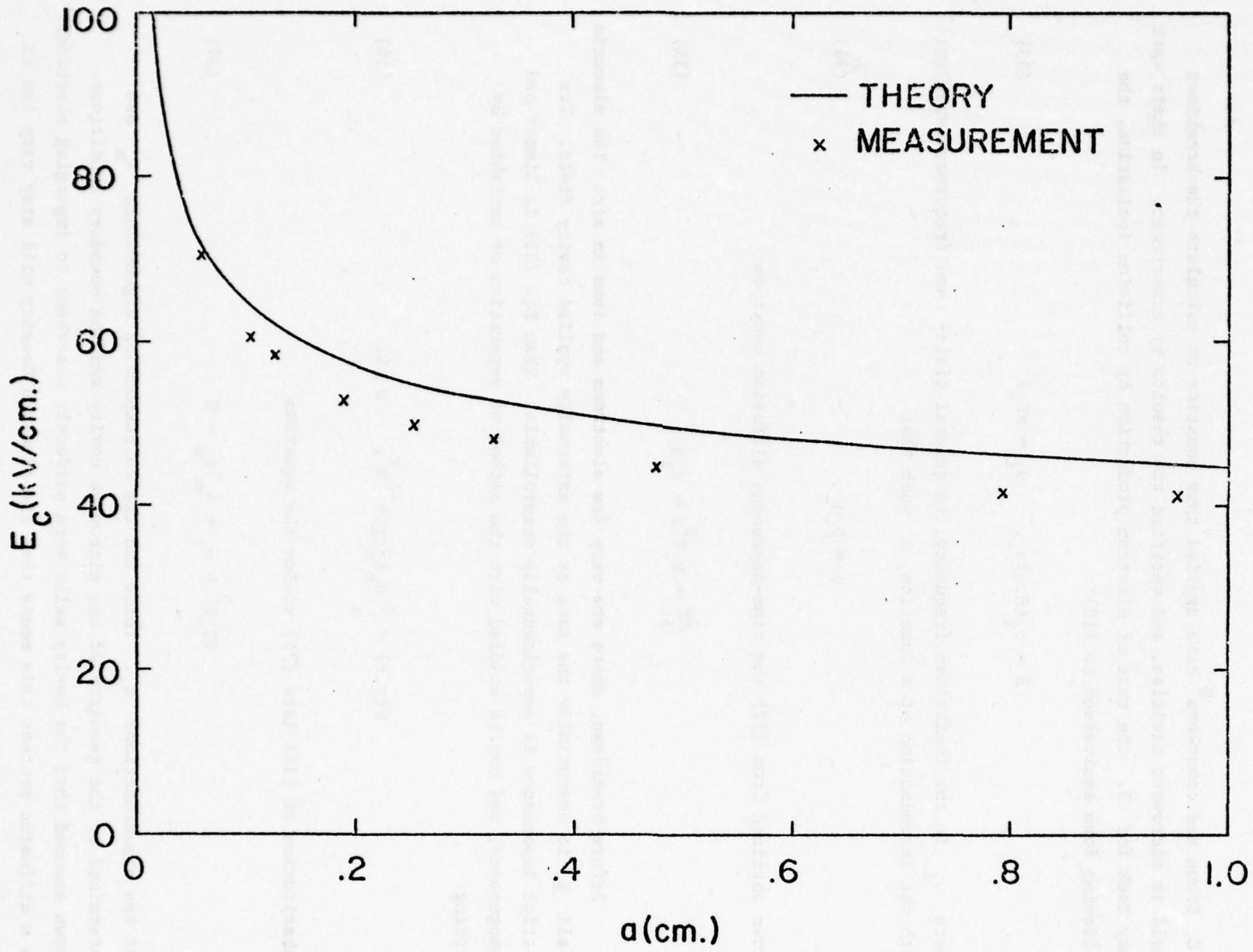


Figure 2. Breakdown electric field E_c in air at normal temperature and pressure as a function of wire radius a. The crosses are data of Peek (ref. 1) taken at 60 Hz.

S.C. Brown and coworkers[8] have applied this equation to calculate the breakdown field in microwave cavities, and verified the results by experiment. In their work they took for S, the rate of electron production by collision ionization, the following form equivalent to (18):

$$S = \nu_i(E,\omega)n_-, \qquad \nu_i = \alpha K_- E \tag{33}$$

where ν_i is the ionization frequency, in general field- and frequency-dependent. With the introduction of a function ψ such that

$$\psi = D_- n_-, \tag{34}$$

Brown obtained from (32) the time-dependent diffusion equation

$$\frac{\partial \psi}{\partial t} = D_- \nabla^2 \psi + \nu_i \psi. \tag{35}$$

Before breakdown, there are very few electrons and ions in air. The electric field $\underline{E}$ is essentially the same as the externally applied cavity field. Its spatial dependence is experimentally controllable. Then Eq. (35) is linear and homogeneous, and can be studied with the method of separation of variables by setting

$$\psi(\underline{r},t) = \sum_m c_m \psi_m(\underline{r}) e^{-\lambda_m t}, \qquad t \geq 0. \tag{36}$$

Substitution of (36) into (35) yields the equation

$$(D_- \nabla^2 + \nu_i + \lambda_m)\psi_m = 0 \tag{37}$$

for the eigenfunctions ψ_m. These and the corresponding eigenvalues λ_m are determined by the geometry of the microwave cavity and the boundary conditions. Brown assumed that the cavity walls were perfectly absorbent to impinging electrons. In a diffusion process this means that the electron density will stay very low in

the vicinity of the wall surface, and will actually extrapolate to zero a short distance behind the wall. Therefore the boundary condition was taken to be

$$\psi_m = 0, \qquad \text{at cavity walls.} \tag{38}$$

This uniquely determines the eigenfunctions and the eigenvalues.

For a general microwave cavity, the breakdown condition can be expressed in terms of the stability of the solution (36). Before breakdown, ψ is stable. This requires that all the eigenvalues λ_m be positive. It is clear that as the breakdown threshold is approached, the eigenvalue spectrum is lowered; and the lowest eigenvalue (say, λ_o) approaches 0. For λ_o only slightly negative, ψ in (36) is unstable and grows exponentially with time. The breakdown criterion is therefore that the lowest eigenvalue be 0 or, equivalently, that the equation

$$(D_- \nabla^2 + \nu_i)\psi_o = 0 \tag{39}$$

have a non-trivial solution.

Herlin and Brown[9] considered Eq. (39) for a coaxial microwave cavity of finite length. The cavity was excited by a definite cavity eigenmode, with definite spatial dependence of the electric field. The breakdown field intensity was measured for the eigenfrequency. Separately, experiments were done to determine the field- and frequency-dependence of the coefficients D_- and ν_i. The data were fed into (39) in the form of empirical formulas. The imposition of the non-triviality condition on the solution led to a transcendental equation for the breakdown field. Ref. 9 should be consulted for calculational details. The calculated breakdown field was found to be in excellent agreement with experiment, making this theory perhaps the most successful breakdown calculation to date.

The above calculation of the microwave breakdown field is analogous to the theoretical determination of the critical mass of a bulk of uranium. Neutrons in a uranium sample diffuse freely, and are scattered, captured and emitted by the uranium nuclei. They initiate nuclear reactions with the nuclei, resulting in the release of huge amounts of energy and daughter neutrons, in much the same way as collision ionization in a gas releases new electrons. The neutron density satisfies a diffusion equation similar to (35). For a uranium sphere with boundary

condition (38), the lowest eigenvalue turns negative when the sphere radius exceeds a certain critical value. The solution becomes unstable, and the neutrons multiply exponentially. A nuclear chain reaction is set off with explosive consequences.

SECTION 4

CALCULATION OF CORONA VOLTAGE-CURRENT CHARACTERISTIC

Consider the coaxial electrode configuration depicted in Fig. 1. When the voltage difference applied across the gap exceeds the critical value, the corona appears on the wire surface. The insulation provided by the air ceases, and a current flows between the wire and the outer cylinder. For practical applications it is important to know the dependence of this corona current on the applied voltage, or the voltage-current characteristic. This section is devoted to its calculation in the quasi-static limit.

As mentioned previously, the corona sheath, which clings to the wire, is a plasma in which electrons and positive ions coexist in comparable concentrations. For a positive corona, the electrons are accelerated towards the wire and the positive ions are repelled towards the cylinder. Thus one expects to find a layer of electrons bound to the wire and a stream of positive ions flowing from the wire to the cylinder. The corona sheath indicates the extent of the electron layer, and the corona current is mainly carried by positive ions. For a negative corona, one would expect the electrons and the positive ions to exchange roles. There is, however, a slight complication: as soon as the electrons leave the sheath and move towards the cylinder, they attach themselves to neutral molecules to form negative ions. Therefore, for the negative corona, the corona current is carried by electrons inside the corona sheath and by negative ions outside.

An important conclusion can be drawn from the above considerations: in the quasi-static limit the corona current is predominantly carried by charges of the same sign as the wire. As an approximation, one neglects the layer of bound charges in the corona current calculations.

4.1 Effect of Ion Mobility

Just as in metallic conduction, the chief determining factor in gaseous conduction is the mobility of the carriers. Taking only this effect into account, one can calculate the d-c corona current for, say, the positive corona from particular cases of Eqs. (9), (11) and (12):

$$\underline{f}_+ = K_+ n_+ \underline{E} \tag{40}$$

$$\nabla \cdot \underline{E} = \frac{e}{\varepsilon_o} n_+ \tag{41}$$

$$\nabla \cdot \underline{f}_+ = 0 \tag{42}$$

These equations describe a time-independent conduction model in which positive ions interact self-consistently with the electric field, but are neither produced nor destroyed by ionization and recombination processes. This model appears to have been first considered by Townsend.[10]

For a cylindrically symmetric geometry, the three equations become

$$f_+ = K_+ n_+ E \tag{43}$$

$$\frac{1}{\rho} \frac{d}{d\rho} (\rho E) = \frac{e}{\varepsilon_o} n_+ \tag{44}$$

$$\frac{1}{\rho} \frac{d}{d\rho} (\rho f_+) = 0 \tag{45}$$

The integration of (45) yields

$$f_+ = \frac{i}{2\pi e \rho} \tag{46}$$

where i is a constant of integration and has the meaning of the corona current per unit length of wire. Elimination of f_+ between (43) and (46) gives

$$e n_+ = \frac{i}{2\pi K_+ \rho E} \tag{47}$$

Substitution of this into the right-hand side of (44) results in the nonlinear differential equation:

$$\frac{d}{d\rho} (\rho E)^2 = \frac{i}{\pi \varepsilon_o K_+} \rho \tag{48}$$

Integration from a to ρ leads to

$$\rho^2 E^2(\rho) = a^2 E^2(a) + \frac{i}{2\pi\varepsilon_o K_+}(\rho^2 - a^2). \tag{49}$$

Solving for $E(\rho)$ and integrating across the gap from a to b, one obtains the voltage difference

$$V = aE(a)\left[\sqrt{(\lambda^2-1)\phi+1} - 1 - \sqrt{1-\phi}\ \ell n\ \frac{\sqrt{1-\phi}+\sqrt{(\lambda^2-1)\phi+1}}{\lambda(\sqrt{1-\phi}+1)}\right] \tag{50}$$

where

$$\lambda = \frac{b}{a}, \qquad \phi = \frac{i}{i_o}, \qquad i_o = 2\pi\varepsilon_o K_+ E^2(a). \tag{51}$$

Eq. (50) is a relation between the applied voltage V, the corona current per unit length of wire i, and the electric field on the wire E(a). In order to arrive at a unique voltage-current characteristic, the last quantity must be determined independently. For this purpose one imposes the corona boundary condition:

$$E(a) = E_c, \qquad \text{after breakdown.} \tag{52}$$

That is to say, the field on the wire does not change with increased applied voltage, but persists at the breakdown value E_c. The system adjusts itself to the increased voltage by emitting an appropriate corona current. With this condition, Eq. (50) becomes

$$V - V_c = \frac{V_c}{\ell n\lambda}\left[\sqrt{(\lambda^2-1)\phi+1} - 1 + (\sqrt{1-\phi} - 1)\ell n\lambda - \sqrt{1-\phi}\ \ell n\left(\frac{\sqrt{1-\phi}+\sqrt{(\lambda^2-1)\phi+1}}{\sqrt{1-\phi}+1}\right)\right] \tag{53}$$

where V_c is the breakdown voltage given by

$$V_c = aE_c\ell n(b/a) \tag{54}$$

for the coaxial configuration.

The corona voltage-current characteristic (53) is plotted in Fig. 3 for the case $\lambda = 100$. Typically $E_c \sim 30$ kV /cm., $K_+ \sim 1$ cm.^{2}/volt sec. From this one has $i_o \sim 0.1$ A/m. Fig. 3 shows that a typical corona current is of the order of 1 mA/m. The curve i versus V has a parabolic shape, and can be fitted closely by the simple form

$$i = \kappa V (V - V_c) \tag{55}$$

This was first obtained by Townsend, and has been periodically verified by experimentalists. Fig. 4 shows some recent data reported by Albrecht, Wagner and Bloss[11] for the positive corona. The measurements were done in pure nitrogen for the coaxial electrode geometry at 1 atmosphere. The current carriers are N^+ ions. The corona voltage-current characteristic is plotted with the current on a logarithmic scale, and compared with the theoretical expression (53). Excellent agreement is indicated.

Fig. 5 shows the radial variations of the electric field $E(\rho)$, the potential $V(\rho)$, and the ion density $n_+(\rho)$ for the case $V = 2V_c$. From Fig. 3, the corresponding corona current is equal to $0.005\, i_o$. The above three quantities are normalized to their respective boundary values E_c, V and n_o, respectively, on the wire where

$$n_o = \frac{\varepsilon_o E_c}{ea} \frac{i}{i_o} . \tag{56}$$

The negative corona voltage-current characteristic can be obtained in a similar fashion. The aforementioned difference in the nature of the negative charge carriers inside the corona sheath from that outside can be accounted for by an effective overall negative ion mobility.

4.2 Effect of Ion Diffusion

In Eq. (40), the part of the particle flux due to diffusion is neglected. This subsection studies the voltage-current characteristic when the diffusion flux is retained. The total flux is therefore given by Eq. (9). In place of Eqs. (43), (44) and (45), one now has

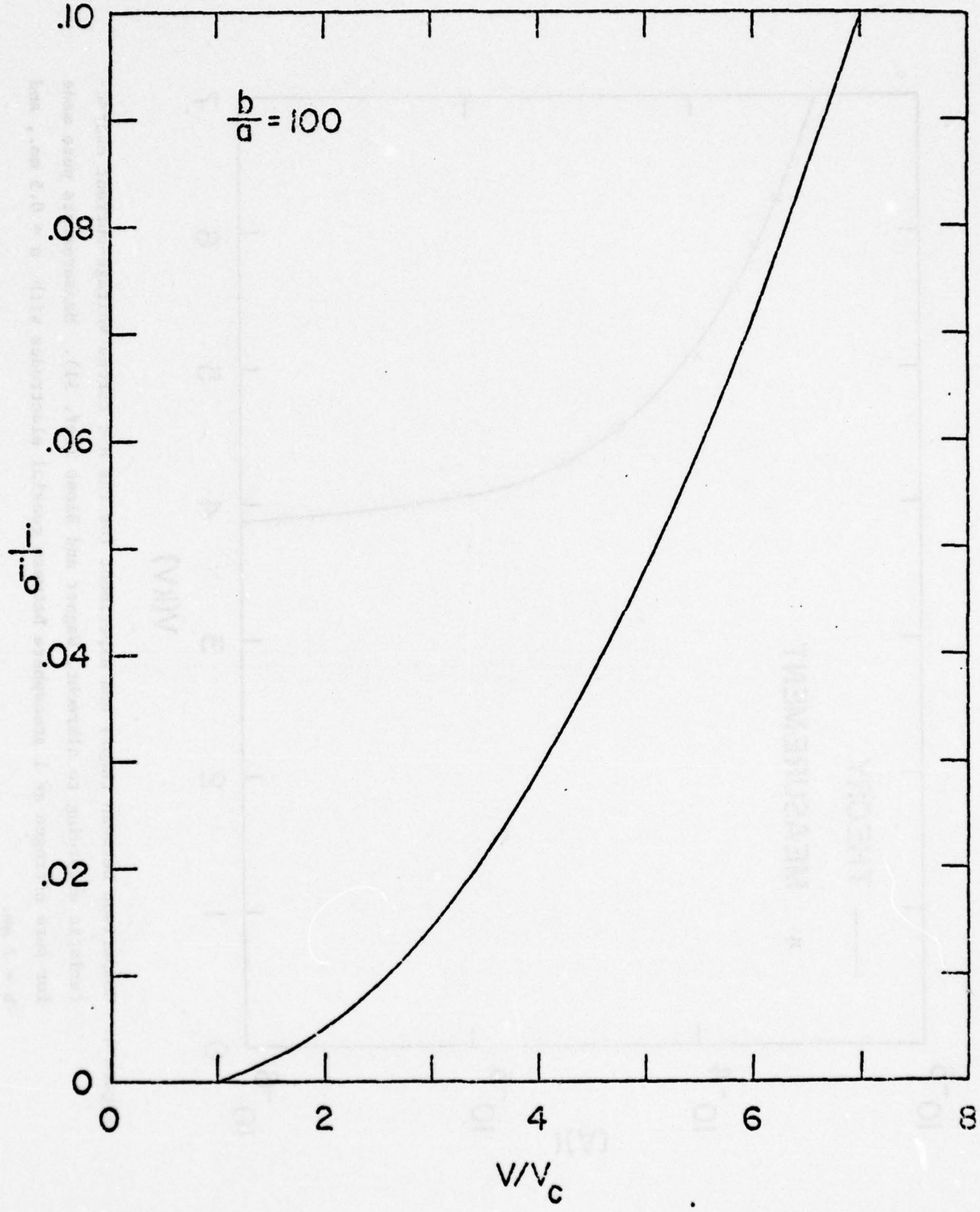


Figure 3. Normalized corona voltage-current characteristic for coaxial electrodes.

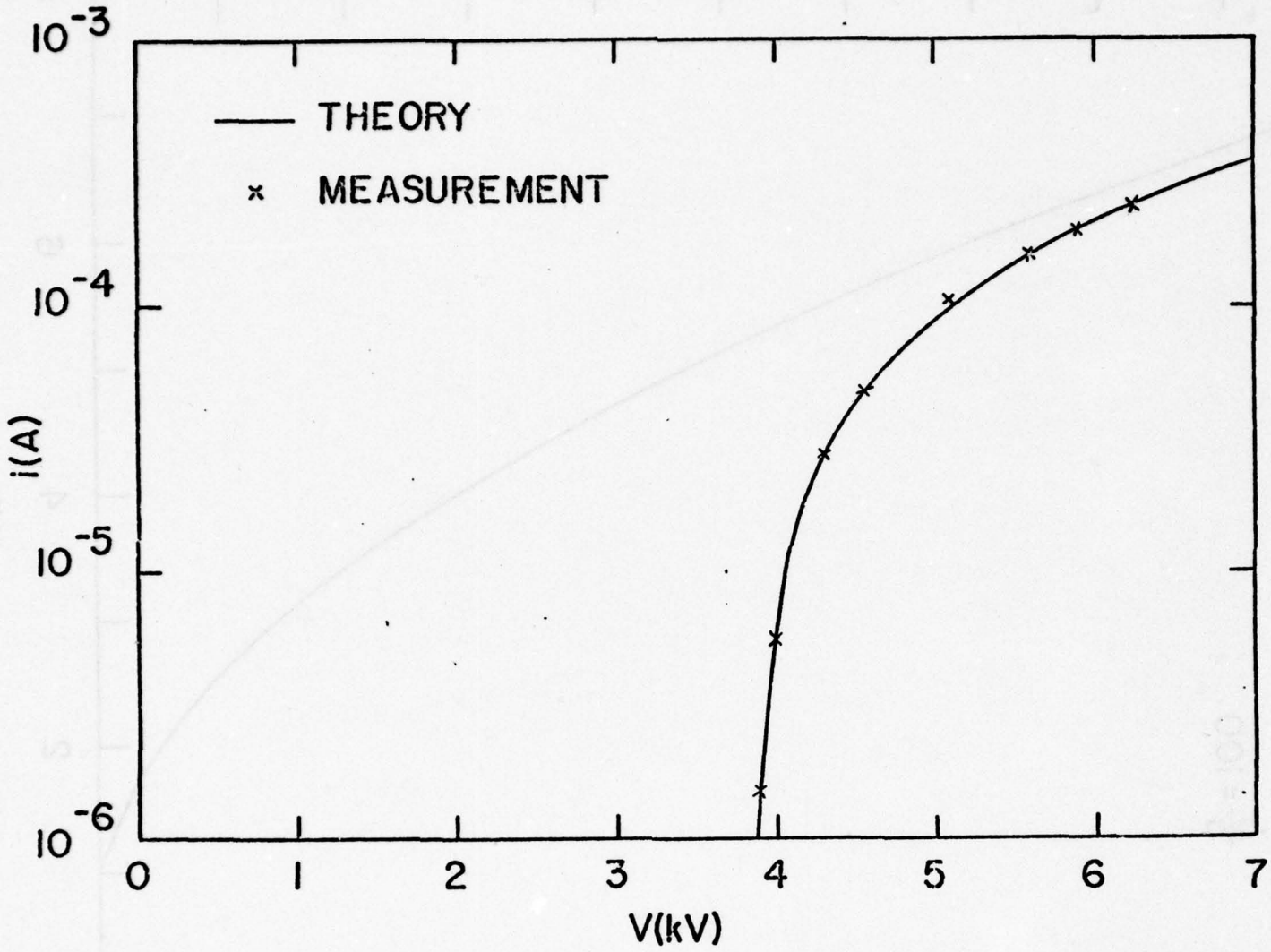


Figure 4. Comparison between theory and experiment for the d-c corona voltage-current characteristic according to Albrecht, Wagner and Bloss (ref. 11). Measurements were made for pure nitrogen at 1 atmosphere between coaxial electrodes with a = 0.5 mm., and b = 7 mm.

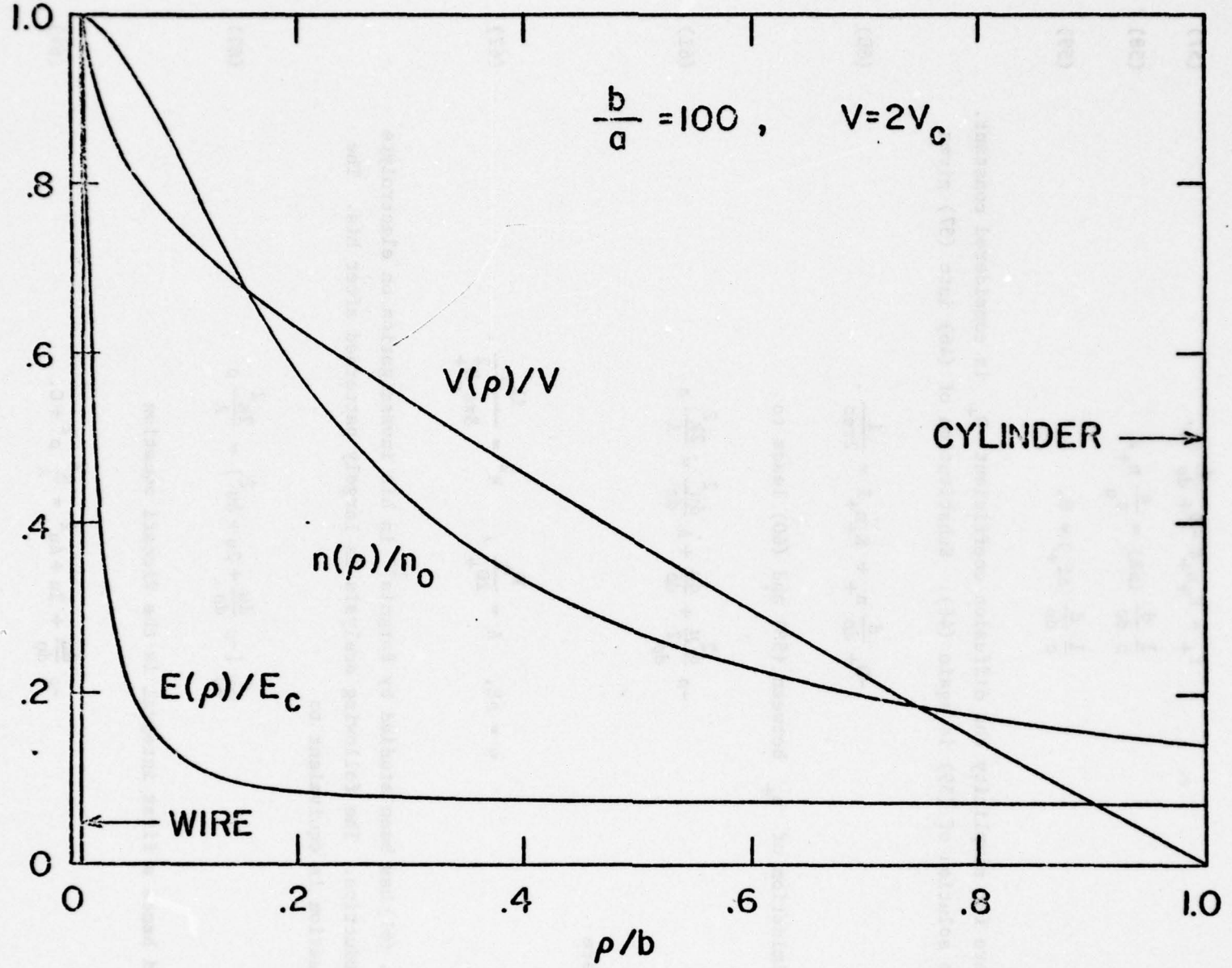


Figure 5. Normalized electric field $E(\rho)$, ion number density $n(\rho)$, and potential $V(\rho)$ across coaxial electrodes in corona with applied voltage difference $V = 2V_c$.

$$f_+ = K_+ n_+ E - D_+ \frac{d}{d\rho} n_+, \tag{57}$$

$$\frac{1}{\rho} \frac{d}{d\rho} (\rho E) = \frac{e}{\varepsilon_o} n_+, \tag{58}$$

$$\frac{1}{\rho} \frac{d}{d\rho} (\rho f_+) = 0, \tag{59}$$

where for simplicity the diffusion coefficient D_+ is considered constant. The solution of (59) is again (46). Substitution of (46) into (57) gives

$$-D_+ \frac{d}{d\rho} n_+ + K_+ n_+ E = \frac{i}{2\pi e\rho} . \tag{60}$$

Elimination of n_+ between (58) and (60) leads to

$$-\rho \frac{d^2u}{d\rho^2} + \frac{du}{d\rho} + \Lambda \frac{du^2}{d\rho} = \frac{2k^2}{\Lambda} \rho \tag{61}$$

where

$$u = \rho E, \quad \Lambda = \frac{K_+}{2D_+} , \quad k^2 = \frac{iK_+}{8\pi\varepsilon_o D_+^2} . \tag{62}$$

Eq. (61) has been studied by Borgnis[12] in his investigation on electrolyte conduction. The following analysis is largely patterned after his. The equation is equivalent to

$$\frac{d}{d\rho} \left[-\rho \frac{du}{d\rho} + 2u + \Lambda u^2\right] = \frac{2k^2}{\Lambda} \rho \tag{63}$$

and hence a first integral is the Riccati equation

$$-\rho \frac{du}{d\rho} + 2u + \Lambda u^2 = \frac{k^2}{\Lambda} \rho^2 + C. \tag{64}$$

With the nonlinear transformation

$$u = -\frac{\rho}{\Lambda}\frac{d}{d\rho}\ell nv, \tag{65}$$

Eq. (64) goes over to a linear equation for the new unknown v:

$$\rho^2\frac{d^2v}{d\rho^2} - \rho\frac{dv}{d\rho} - (k^2\rho^2 + \Lambda C)v = 0. \tag{66}$$

This is a modified Bessel equation, and the solution is

$$v = \rho[C'I_\nu(k\rho) + C''K_\nu(k\rho)], \tag{67}$$

where

$$\nu = \sqrt{1+\Lambda C}. \tag{68}$$

The electric field is obtainable from (62) and (65) as

$$E = -\frac{1}{\Lambda}\frac{d}{d\rho}\ell nv. \tag{69}$$

The solution contains three unknown constants C', C" and ν. Since only ℓnv appears in (69), it is clear that only the ratio C'/C" matters. This still leaves one with two constants--one more than E(a) in the previous subsection. The reason is that the introduction of the diffusion term in Eq. (60) increases the order of the differential equation by 1. An extra boundary condition pertinent to the diffusion process must be stipulated. Instead of seeking such an extra diffusion condition, which is often difficult to establish, a different approach will be adopted here. It will be assumed that the correction due to diffusion is small (as is amply indicated by the good agreement of the results in Subsection 4.1 with experiment), so that, in the limit $D_+ \to 0$, the solution should tend continuously to the previous diffusion-free expression. It can be shown that

for a positive corona, the function I_ν in (67) should be eliminated. This essentially gets rid of the extra constant of integration. Therefore one obtains for the electric field

$$E = -\frac{1}{\Lambda}\frac{d}{d\rho}\,\ell n[\rho K_\nu(k\rho)]. \tag{70}$$

Integration over ρ from a to b yields the voltage difference

$$V = \frac{1}{\Lambda}\,\ell n\left[\frac{aK_\nu(ka)}{bK_\nu(kb)}\right]. \tag{71}$$

The surviving unknown constant ν is determined from the corona boundary condition (52) which by (70) reads

$$-\frac{kaK'_\nu(ka)}{K_\nu(ka)} = \Lambda aE_c + 1. \tag{72}$$

Eqs. (71) and (72) together constitute the corona voltage-current characteristic with diffusion.

It can be shown that, in the limit $D_+ \to 0$, all three constants Λ, k and ν diverge. One can therefore use the Debye asymptotic formulas for large order

$$K_\nu(\nu z) \sim \sqrt{\frac{\pi}{2\nu}}\,\frac{1}{(1+z^2)^{1/4}}\,e^{-\nu\zeta}, \qquad K'_\nu(\nu z) \sim -\sqrt{\frac{\pi}{2\nu}}\,\frac{(1+z^2)^{1/4}}{z}\,e^{-\nu\zeta} \tag{73}$$

where

$$\zeta = \sqrt{1+z^2} + \ell n\frac{z}{1+\sqrt{1+z^2}}. \tag{74}$$

Substitution of (73) into (72) yields the simple solution

$$\nu = \sqrt{[\Lambda aE_c+1]^2 - k^2a^2}. \tag{75}$$

In terms of the reduced corona current $\phi = i/i_o$ introduced in (51), one finds

$$(ka)^2 = (\Lambda aE_c)^2\phi. \tag{76}$$

Hence

$$\nu = \Lambda a E_c \sqrt{(1+\delta)^2 - \phi}, \qquad \delta = \frac{1}{\Lambda a E_c} . \tag{77}$$

In the Debye asymptotic limit, the voltage difference (71) reduces to

$$V = \frac{1}{\Lambda}\left[\sqrt{\nu^2+(kb)^2} - \sqrt{\nu^2+(ka)^2} - \nu \ell n\left(\frac{a}{b} \cdot \frac{\nu+\sqrt{\nu^2+(kb)^2}}{\nu+\sqrt{\nu^2+(ka)^2}}\right)\right] \tag{78}$$

From Eqs. (75), (76) and (77), it can be seen that (78) differs from (50) only by the presence of the quantity δ in (77). By (62) and (77), one obtains

$$\delta = \frac{2D_+}{K_+ a E_c} . \tag{79}$$

In air $D_+ \sim 0.028$ cm.^{2}/sec., $K_+ \sim 1.36$ cm.^{2}/volt sec., and so $\Lambda = K_+/2D_+ \sim 24$/volt. It then turns out that $\delta \sim 10^{-6}$, which is entirely negligible compared to 1 in (77). Therefore it is concluded that the effect of diffusion is infinitesimal in the present case compared to that of mobility, although the former actually overtakes the latter in the microwave regime.

The effect of diffusion on the voltage-current characteristic has also been studied by Chekmarev,[13] but with a boundary condition other than (52).

4.3 Effect of Ionization

The two calculations of the corona voltage-current characteristic presented above are based on the assumption that the current is carried by charges of one sign emitted by the wire. This is called the unipolar theory. In reality, since the corona sheath contains charges of both signs created by ionization, both types of charges must participate in conduction. For example, in a positive corona, some of the electrons in the sheath will be attracted to the positive wire and migrate towards it, forming a small electron current. A calculation which takes this aspect into account is a bipolar theory.

There is as yet no reliable quantitative theory for the state of affairs inside the corona sheath. The precise ionization and recombination rates and the detailed field and charge distributions inside the sheath are difficult to evaluate. In the following calculations the effect of ionization will be represented by a constant overall ionization rate. Therefore, although the boundary-value problem so formulated can be solved exactly, the results can be expected to have only qualitative and methodological values. With the total neglect of diffusion justifiable from the results of the last subsection, the basic equations are

$$\underline{f}_+ = K_+ n_+ \underline{E}, \qquad \underline{f}_- = -K_- n_- \underline{E}, \tag{80}$$

$$\nabla \cdot \underline{E} = \frac{e}{\varepsilon_o} (n_+ - n_-), \tag{81}$$

$$\nabla \cdot \underline{f}_+ = S, \qquad \nabla \cdot \underline{f}_- = S \tag{82}$$

where S is a constant ionization rate. In the case of axial symmetry, these equations become

$$f_+ = K_+ n_+ E, \qquad f_- = -K_- n_- E \tag{83}$$

$$\frac{1}{\rho} \frac{d}{d\rho} (\rho E) = \frac{e}{\varepsilon_o} (n_+ - n_-) \tag{84}$$

$$\frac{1}{\rho} \frac{d}{d\rho} (\rho f_+) = S, \qquad \frac{1}{\rho} \frac{d}{d\rho} (\rho f_-) = S. \tag{85}$$

The solutions of (83) and (85) are

$$\rho K_+ n_+ E = \frac{1}{2} S\rho^2 + C, \qquad K_+ n_+ E + K_- n_- E = \frac{i}{2\pi e \rho} \tag{86}$$

where C and i are constants of integration, and i again has the meaning of the corona current per unit length of wire. For a positive corona, the negative charges are created by ionization in the space between the electrodes and migrate towards the wire. The density of negative charges n_- at the outer cylinder $\rho = b$ can be set equal to 0. This boundary condition determines C. Therefore the solution (86) becomes

$$\rho K_+ n_+ E = \frac{i}{2\pi e} - \frac{S}{2}(b^2-\rho^2), \qquad \rho K_- n_- E = \frac{S}{2}(b^2-\rho^2). \tag{87}$$

Solving for n_+ and n_- and substituting into (84), one obtains the differential equation

$$\rho E \frac{d}{d\rho}(\rho E) = \frac{i}{2\pi\varepsilon_o K_+}\rho - \frac{eS}{2\varepsilon_o}\left(\frac{1}{K_+}+\frac{1}{K_-}\right)(b^2-\rho^2)\rho. \tag{88}$$

Integrating from a to ρ, one obtains

$$(\rho E)^2 = (aE_c)^2 + \frac{i}{2\pi\varepsilon_o K_+}(\rho^2-a^2) - \frac{eS(K_+ + K_-)}{2\varepsilon_o K_+ K_-}\left[b^2(\rho^2-a^2) - \frac{1}{2}(\rho^4-a^4)\right] \tag{89}$$

where one has imposed the corona boundary condition (52), namely, that the electric field on the wire surface is maintained at the critical value E_c after breakdown. Solving (89) for E, and integrating over ρ from a to b, one arrives at the following voltage-current characteristic

$$V = aE_c\int_a^b \frac{d\rho}{\rho}\sqrt{1+\phi\left(\frac{\rho^2}{a^2}-1\right) - SW(\rho)} \tag{90}$$

where $\phi = i/i_o$ as in (51), and

$$W(\rho) = \frac{e(K_+ + K_-)}{2\varepsilon_o a^2 E_c^2 K_+ K_-}\left[b^2(\rho^2-a^2) - \frac{1}{2}(\rho^4-a^4)\right]. \tag{91}$$

For $S = 0$, Eq. (90) reduces to the ionizationless limit (53). For nonzero S, the integral can also be worked out analytically. But the result will be very complicated. Since ionization effects are only very approximately incorporated in (85), an exhaustive calculation will be quite out of place here. There is, at any rate, no dependable method to assign an effective value to S. A qualitative examination of (90) suffices. It is observed that the function $W(\rho)$ is positive inside the range of integration. The effect of ionization is therefore to decrease the expression under the square root. This decrease must be compensated

by an increase in ϕ (or the corona current i) if the voltage difference V is to remain the same. One therefore arrives at the intuitively obvious conclusion that ionization augments the corona current.

SECTION 5

APPLICATION TO A SINGLE LINE ABOVE GROUND

In the previous sections, a number of boundary-value problems in the study of the electrical corona on a long wire were solved for the coaxial electrode configuration illustrated in Fig. 1. This geometry was favored because its high degree of symmetry facilitates the mathematics, and because experimental data for it are available for comparison with calculation. In practice there exists another configuration of great importance, consisting of a long wire parallel to the surface of a ground plane. This is, for example, the geometry of the high-voltage power line. As is well known, if the ground plane is perfectly conducting, this geometry is also equivalent to that of two parallel wires operating in the push-pull mode and far away from other conductors.

This section calculates the corona voltage-current characteristic for the wire-and-plane configuration. The results are applied to study the corona effect on large signal propagation along a semi-infinite wire above ground.

5.1 Corona Voltage-Current Characteristic

Consider a long straight wire of radius a whose axis lies at a height h above a perfectly conducting ground plane, as depicted in Fig. 6. Suppose the wire is charged to a potential V relative to ground. When V exceeds the corona onset value V_c, a current will flow through the air between the wire and the ground. The critical potential V_c is related to the breakdown field E_c through Eq. (4). As has been discussed in Section 3, E_c is a function of a and not of h. It is for all practical purposes the same as for the coaxial geometry.

The coordinate system most suitable for studying the wire-and-ground configuration in Fig. 6 is that of the bipolar coordinates (ξ,η,z). The relations between (x,y) and (ξ,η) are

$$(x - d \cot \eta)^2 + y^2 = d^2 \csc^2 \eta, \tag{92}$$

$$x^2 + (y - d \coth \xi)^2 = d^2 \operatorname{csch}^2 \xi. \tag{93}$$

The parameter d is a positive constant. The range of ξ is from $-\infty$ to ∞,

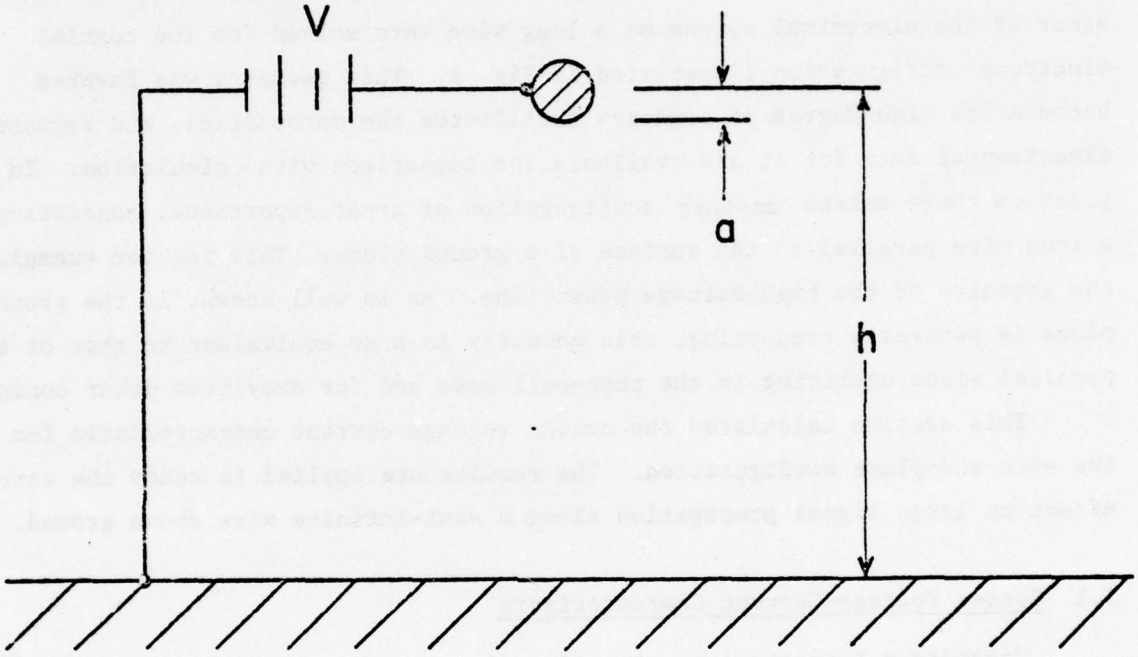


Figure 6. Wire-over-plane electrode configuration for corona study.

and that for η from 0 to 2π. Then these relations describe two families of orthogonally intersecting circles on the x-y plane as shown in Fig. 7. Eq. (92) represents a family of circles with centers on the x-axis and passing through two common points $y = \pm d$ known as the foci. Each circle is labeled by a value of η. Eq. (93) represents the orthogonal net. Each of its circles is labeled by a value of ξ. The upper focus is the limit $\xi \to -\infty$, and the x-axis the limit $\xi \to 0$. The circles with $\xi > 0$ are below the x-axis. Note that $\eta = \pi$ for $x = 0$, $-d < y < d$, that is, along the interfocal line.

The wire in Fig. 6 can be represented by one of the circles (93). Let it be labeled by a value $\xi_o < 0$. It can be shown that

$$\xi_o = -\cosh^{-1}\left(\frac{h}{a}\right), \qquad d = \sqrt{h^2 - a^2}. \tag{94}$$

The coordinate η measures the angle around the wire.

In the following corona current calculations, only the effect of ion mobility will be considered. The basic equations are the same as Eqs. (40), (41) and (42) in Subsection 4.1:

$$\underline{f}_+ = K_+ n_+ \underline{E}, \tag{95}$$

$$\nabla \cdot \underline{E} = \frac{e}{\varepsilon_o} n_+, \tag{96}$$

$$\nabla \cdot \underline{f}_+ = 0. \tag{97}$$

If the wire is thin, the state of affairs close to the wire may be considered axially symmetric, so that the family of ξ-labeled circles are equipotential surfaces. The corona current flows from wire to ground along circles of constant η in Fig. 7. This means that $\underline{f}_+$ and $\underline{E}$ have only ξ-components. Writing out the above equations in bipolar coordinates, one obtains

$$f_+ \hat{e}_\xi = K_+ n_+ E \hat{e}_\xi, \tag{98}$$

$$\frac{(\cosh\xi - \cos\eta)^2}{d^2} \frac{\partial}{\partial \xi}\left(\frac{d}{\cosh\xi - \cos\eta} E\right) = \frac{e}{\varepsilon_o} n, \tag{99}$$

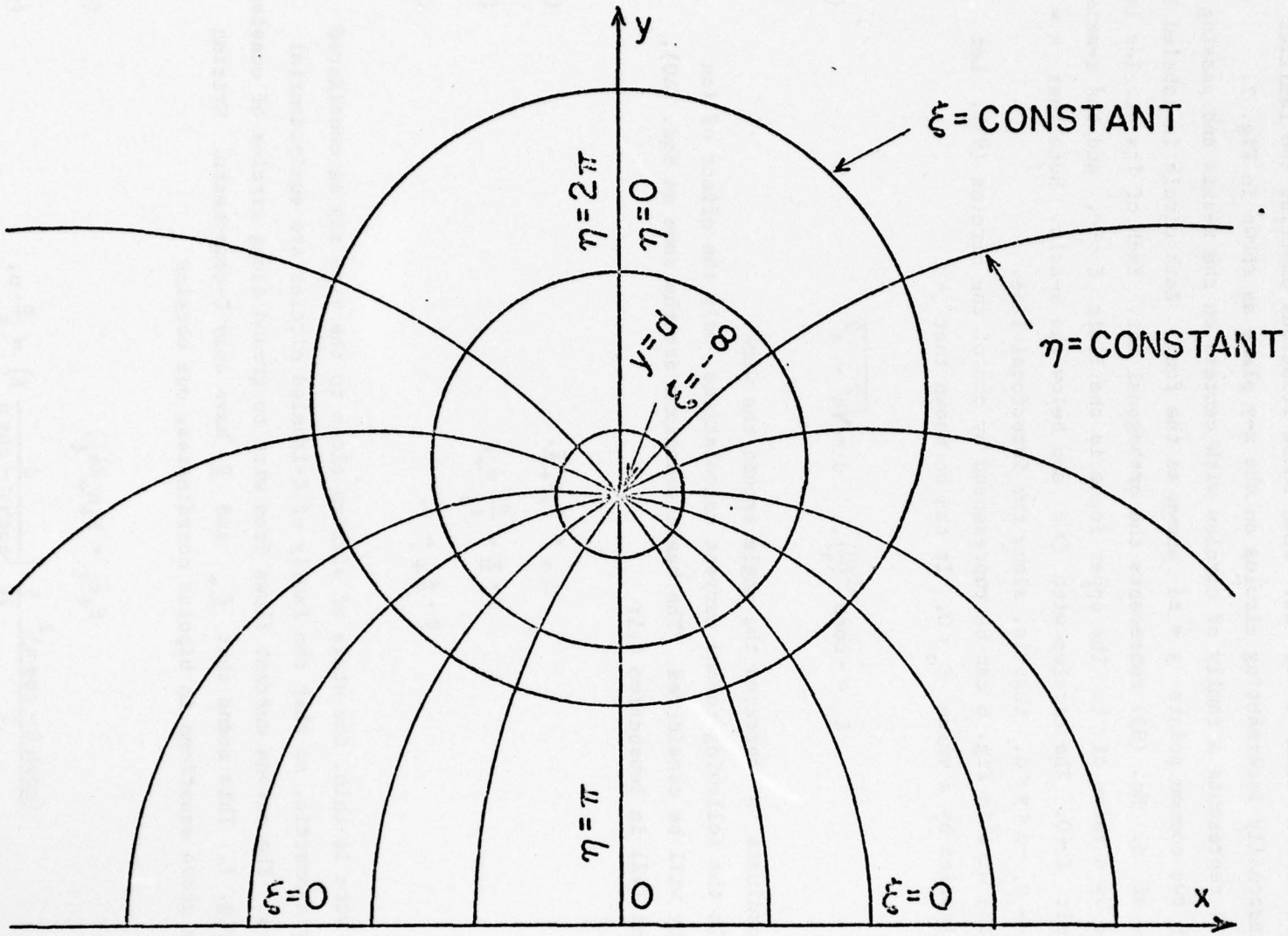


Figure 7. Bipolar coordinates.

$$\frac{(\cosh \xi - \cos \eta)^2}{d^2} \frac{\partial}{\partial \xi} \left(\frac{d}{\cosh \xi - \cos \eta} f_+ \right) = 0. \tag{100}$$

The solution of (100) is

$$f_+ = \frac{\cosh \xi - \cos \eta}{d} C(\eta) \tag{101}$$

where $C(\eta)$ depends only on η. For a thin-wire the corona current flowing out from the wire surface is isotropic. This means that

$$f_+ = \frac{i}{2\pi e a}, \quad \text{at} \quad \xi = \xi_o \tag{102}$$

where, as before, i is the corona current per unit length of wire. Under this boundary condition, Eq. (101) becomes

$$f_+ = \frac{i}{2\pi e a} \frac{\cosh \xi - \cos \eta}{\cosh \xi_o - \cos \eta}. \tag{103}$$

Solving for n_+ from (98) and (103) and substituting in (99), one obtains

$$\frac{\partial}{\partial \xi} \left(\frac{d}{\cosh \xi - \cos \eta} E \right)^2 = \frac{i}{\pi \epsilon_o K_+} \frac{d}{a(\cosh \xi_o - \cos \eta)} \left(\frac{d}{\cosh \xi - \cos \eta} \right)^2. \tag{104}$$

Integration from ξ_o to ξ yields

$$\left(\frac{d}{\cosh \xi - \cos \eta} E \right)^2 = \left(\frac{d}{\cosh \xi_o - \cos \eta} E_c \right)^2 + \frac{i}{\pi \epsilon_o K_+} \frac{d^3}{a(\cosh \xi_o - \cos \eta)} \int_{\xi_o}^{\xi} \frac{d\xi}{(\cosh \xi - \cos \eta)^2}, \tag{105}$$

where one has already imposed the corona boundary condition (52), that is, $E = E_c$ at $\xi = \xi_o$.

In bipolar coordinates, the ξ-component of the field is related to the potential through

$$E = -\frac{\cosh\xi - \cos\eta}{d}\frac{\partial V}{\partial \xi}, \tag{106}$$

and so the left-hand side of (105) is simply the square of $\partial V/\partial\xi$. The voltage difference can be obtained by integrating this last derivative from the wire to the ground. The path of integration is most conveniently chosen as the interfocal line $\eta = \pi$. With this choice the integral in (105) becomes

$$\int_{\xi_o}^{\xi} \frac{d\xi}{(\cosh\xi + 1)^2} = \int_{\xi_o}^{\xi} \frac{d\xi}{4\cosh^4(\xi/2)} = \frac{1}{2}\left[\tanh\left(\frac{\xi}{2}\right) - \frac{1}{3}\tanh^3\left(\frac{\xi}{2}\right)\right]_{\xi_o}^{\xi}. \tag{107}$$

Also, by (94),

$$\frac{d}{\cosh\xi_o + 1} = a\sqrt{\frac{h-a}{h+a}}. \tag{108}$$

With these simplifications, the voltage difference between wire and ground becomes

$$V = aE_c\int_{\xi_o}^{o} d\xi \left\{\frac{h-a}{h+a} + \phi\left(\frac{h^2}{a^2} - 1\right)\sqrt{\frac{h-a}{h+a}}\,[\chi(\xi) - \chi(\xi_o)]\right\}^{\frac{1}{2}} \tag{109}$$

where $\phi = i/i_o$ as in (51), and

$$\chi(\xi) = \tanh\left(\frac{\xi}{2}\right) - \frac{1}{3}\tanh^3\left(\frac{\xi}{2}\right). \tag{110}$$

Just at breakdown, $V = V_c$ and $\phi = 0$. Eq. (109) gives

$$V_c = -\xi_o aE_c\sqrt{\frac{h-a}{h+a}}, \tag{111}$$

or, by (94),

$$V_c = aE_c \sqrt{\frac{h-a}{h+a}} \cosh^{-1}\left(\frac{h}{a}\right) \tag{112}$$

which is essentially (4) for $h \gg a$.

The wire-to-ground corona voltage-current characteristic (109) is computed for the case $h/a = 100$ and plotted in Fig. 8. It has the same parabolic appearance as that in Fig. 3 for the coaxial geometry, and can also be fitted by the simple expression (55). In fact, it is obvious from (109) that for a large current ($\phi \to \infty$), one has $\phi \sim V^2$. Compared to the curve in Fig. 3 with $b/a = 100$, the present curve lies slightly lower.

5.2 Corona Effect on Large Signal Propagation

Consider a semi-infinite straight wire of radius a hung over a perfectly conducting ground plane at a height h, as illustrated in Fig. 9. It is taken to stretch from $z = 0$ to ∞. Let the wire be quiescent for $t < 0$. If, starting at $t = 0$, a voltage difference $V_g(t)$ is applied between the free end of the wire and the ground by a generator, the signal will propagate down the line to infinity. To a good approximation, the propagation is described by the pair of transmission line equations:

$$\frac{\partial V}{\partial z} = -L \frac{\partial I}{\partial t}, \qquad \frac{\partial I}{\partial z} = -C \frac{\partial V}{\partial t} \tag{113}$$

where V is the shunt voltage, I the series current, and L and C are, respectively, the inductance and capacitance per unit length of line. For $h \gg a$, one has

$$L = \frac{\mu_o}{4\pi} 4\ell n\left(\frac{2h}{a}\right), \qquad C = 4\pi\varepsilon_o \left[4\ell n\left(\frac{2h}{a}\right)\right]^{-1}. \tag{114}$$

If the signal exceeds the breakdown voltage V_c for the wire, coronas will be formed along its path. Current will flow from the wire to the ground, forming

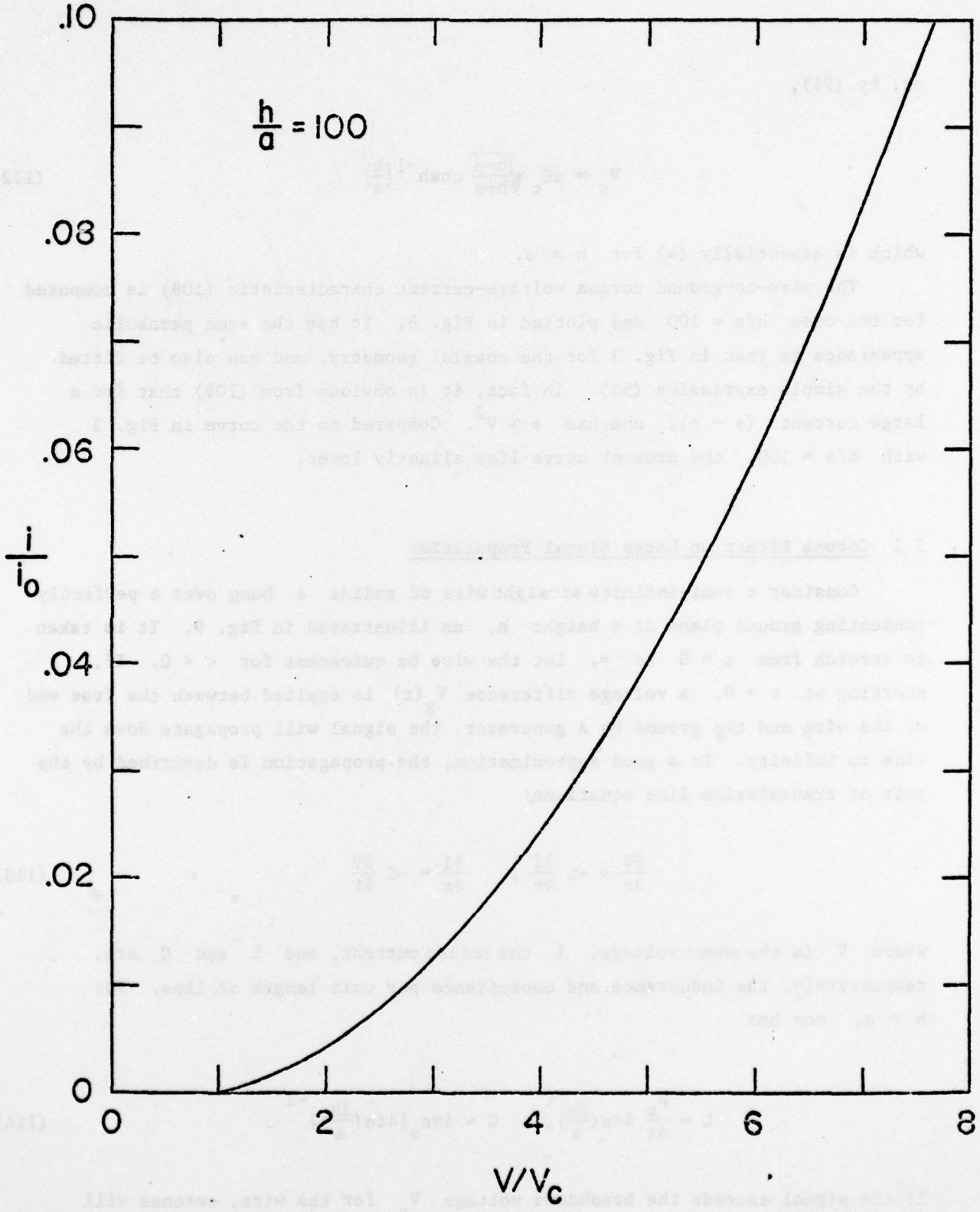


Figure 8. Normalized corona voltage-current characterisitic for wire-and-plane electrodes.

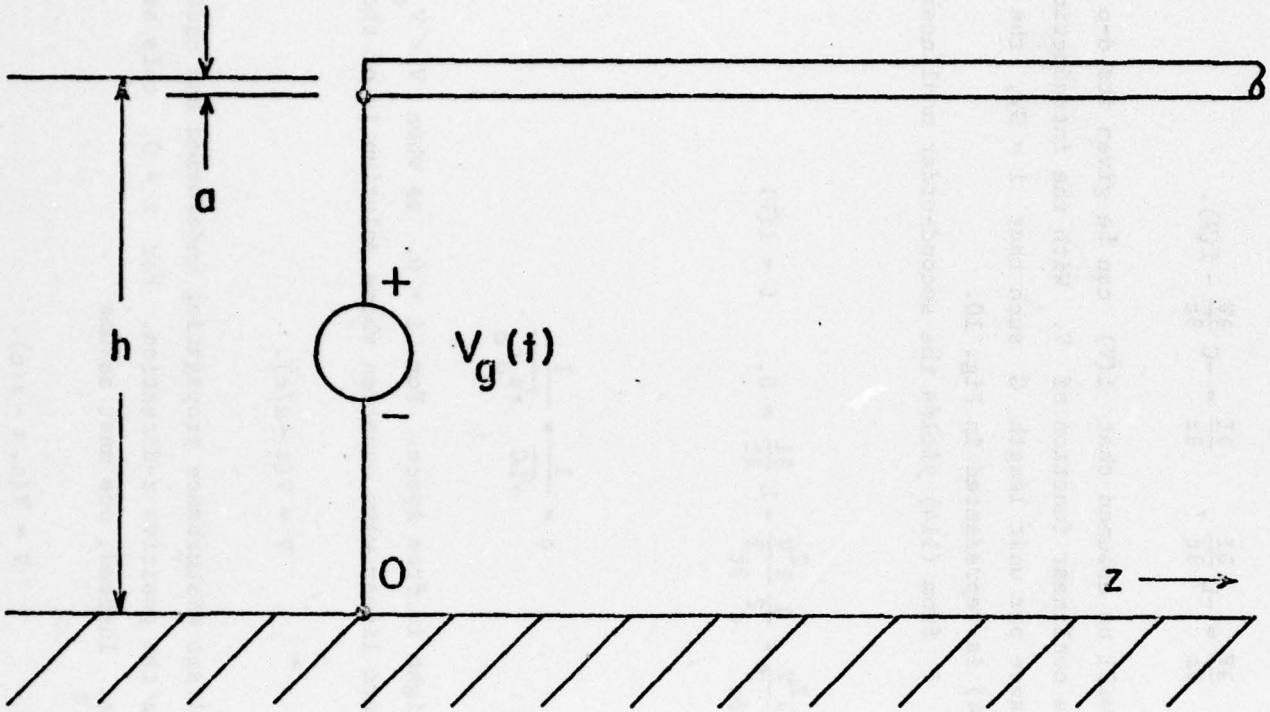


Figure 9. Semi-infinite transmission line over a ground plane.

a leakage and a loss. In this event, the transmission line equations (113) must be corrected by a corona shunt current per unit length $i(V)$:

$$\frac{\partial V}{\partial z} = -L \frac{\partial I}{\partial t}, \qquad \frac{\partial I}{\partial z} = -C \frac{\partial V}{\partial t} - i(V). \tag{114}$$

In the following it will be assumed that $i(V)$ can be given its d-c value from Eq. (109). This is a nonlinear function of V. With the introduction of a corona shunt conductance per unit length G such that $i = GV$, the equivalent circuit for Eqs. (114) is represented in Fig. 10.

Elimination of I from (114) yields the second-order nonlinear wave equation for V:

$$\frac{\partial^2 V}{\partial z^2} - \frac{1}{c^2} \frac{\partial^2 V}{\partial t^2} - L \frac{\partial i}{\partial t} = 0, \qquad i = i(V) \tag{115}$$

where

$$c = \frac{1}{\sqrt{LC}} = \frac{1}{\sqrt{\mu_o \varepsilon_o}} \tag{116}$$

is the velocity of light in free space. For $i = 0$, as when $V < V_c$, Eq. (115) reduces to the standard linear wave equation whose solution is of the form

$$V = V(t - z/c). \tag{117}$$

This represents a voltage disturbance propagating undeformed and undamped with the speed of light in the positive z-direction. For $i \neq 0$, this simple form is no longer adequate. Instead, one must assume

$$V = V(z, t - z/c). \tag{118}$$

This added direct dependence on z accounts for the distortion of the signal due to the formation of coronas along the line. It is convenient to change the independent variables from the set (z,t) to the set (z,τ) with

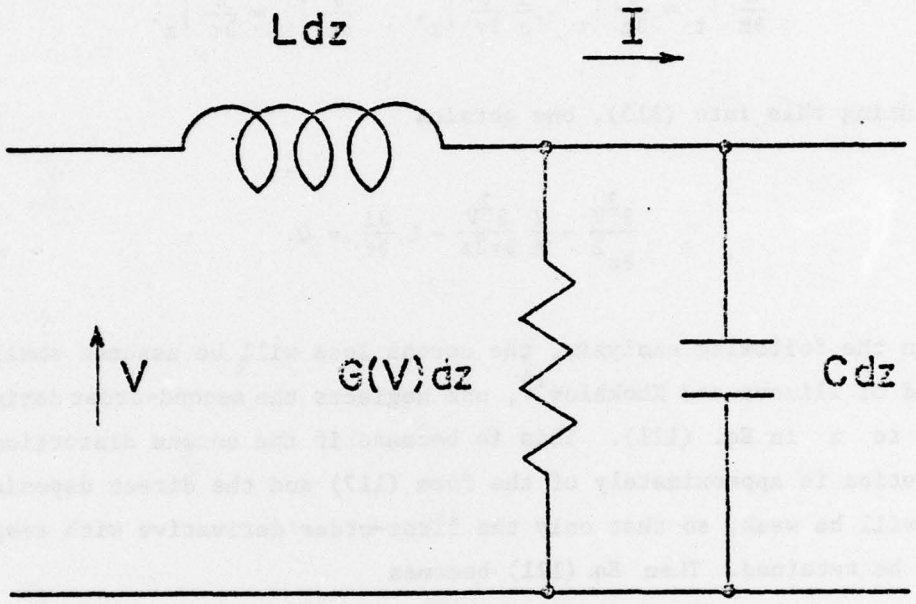


Figure 10. Equivalent circuit for transmission line, with corona loss represented by nonlinear shunt conductance per unit length G(V).

$$\tau = t - z/c, \tag{119}$$

whereby

$$\frac{\partial}{\partial z}\Big|_t = \frac{\partial}{\partial z}\Big|_\tau - \frac{1}{c}\frac{\partial}{\partial \tau}\Big|_z, \qquad \frac{\partial}{\partial t}\Big|_z = \frac{\partial}{\partial \tau}\Big|_z. \tag{120}$$

Substituting this into (115), one obtains

$$\frac{\partial^2 V}{\partial z^2} - \frac{2}{c}\frac{\partial^2 V}{\partial \tau \partial z} - L\frac{\partial i}{\partial \tau} = 0. \tag{121}$$

In the following analysis, the corona loss will be assumed small. Following a method of Ilinova and Khokhlov[14], one neglects the second-order derivative with respect to z in Eq. (121). This is because if the corona distortion is small, the solution is approximately of the form (117) and the direct dependence on z will be weak, so that only the first-order derivative with respect to z need be retained. Then Eq. (121) becomes

$$\frac{\partial}{\partial \tau}\left(\frac{2}{c}\frac{\partial V}{\partial z} + Li\right) = 0, \tag{122}$$

with the solution

$$\frac{2}{c}\frac{\partial V}{\partial z} + Li = C(z) \tag{123}$$

where C is function of z alone. Eq. (123) holds for all τ. If the line is unexcited for $t < 0$, one must conclude that $C(z) = 0$. Introducing the characteristic impedance Z_c of the line, such that

$$Z_c = cL = \sqrt{\frac{L}{C}} = \sqrt{\frac{\mu_o}{\varepsilon_o}}\,\frac{1}{\pi}\,\ell n\left(\frac{2h}{a}\right), \tag{124}$$

one can rewrite (123) as

$$\frac{\partial V}{\partial z} + \frac{1}{2} Z_c i(V) = 0. \tag{125}$$

For a given functional dependence of i on V, the integration of this equation is straightforward. One assumes here for simplicity the parabolic form (55):

$$i(V) = \begin{cases} 0 & V < V_c \\ \kappa V(V - V_c) & V > V_c \end{cases}. \tag{126}$$

The constant κ can be adjusted to fit Eq. (109) or Fig. 8. Then the solution of (125) is

$$V(z,\tau) = \begin{cases} f(\tau) & V < V_c \\ \dfrac{V_c}{1 - g(\tau)\exp\left(-\frac{1}{2} Z_c \kappa V_c z\right)} & V > V_c \end{cases} \tag{127}$$

where $f(\tau)$ and $g(\tau)$ are some functions of τ alone, to be determined by boundary conditions.

Suppose the generator in Fig. 9 puts out a voltage pulse of the double-exponential form:

$$V_g(t) = V_o\left(e^{-\alpha t} - e^{-\beta t}\right)\theta(t), \tag{128}$$

and suppose that V_o is sufficiently large that $V_g(t)$ exceeds the breakdown voltage V_c for $\tau' < t < \tau''$, as shown in Fig. 11. The unknown functions $f(\tau)$ and $g(\tau)$ in (127) will be determined by matching the solution $V(z,\tau)$ with the boundary value (128) at the driving point $z = 0$ of the line. At this point, τ is equal to t, and (127) becomes

$$V(0,t) = \begin{cases} f(t) & V < V_c \\ \dfrac{V_c}{1 - g(t)} & V > V_c \end{cases}. \tag{129}$$

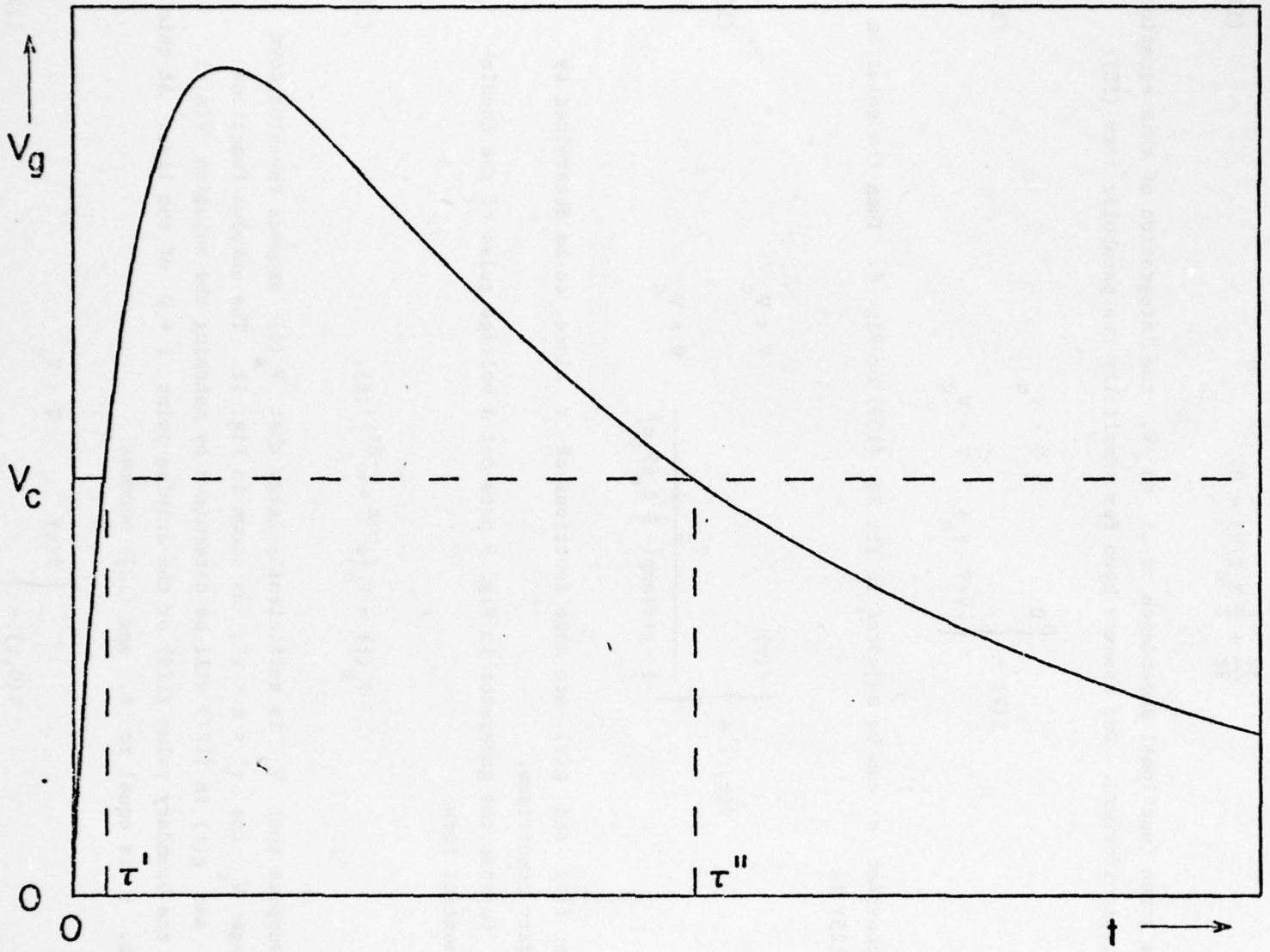


Figure 11. Example of a double-exponential voltage pulse with peak value exceeding the corona onset voltage V_c.

Equating this with $V_g(t)$ in (128) yields the complete solution for general z and τ:

$$V(z,\tau) = \begin{cases} V_g(\tau) & 0 \le \tau \le \tau', \\ \dfrac{V_c}{1 - \left[1 - \dfrac{V_c}{V_g(\tau)}\right] \exp\left(-\frac{1}{2} Z_c \kappa V_c z\right)} & \tau' \le \tau \le \tau'', \\ V_g(\tau) & \tau'' \le \tau \le \infty. \end{cases} \tag{130}$$

This result is easy to interpret. The portions of the pulse in Fig. 11 below τ' and above τ'', being sub-critical, will propagate unaltered and unattenuated down the line with the speed of light. The portion between τ' and τ'' will be distorted by corona, and will be leveled down to V_c at a sufficiently large distance z from the voltage input for which the exponential factor in (130) is small. The velocity of propagation and the width of this portion are unaffected. This result can readily be extended to any general pulse input other than (128): all supercritical portions of the pulse will eventually be chopped down by corona to the critical value.

The order of magnitude of the propagation distance, at which corona attenuation is appreciable, can be estimated from the damping constant $Z_c \kappa V_c$ in (130). Typically this quantity has a value $\sim 10^{-6}$/meter. Thus the pulse has to travel some 1000 kilometers before corona attenuation becomes severe. The reason for the smallness of the effect is not hard to find. The corona onset voltage is usually very high. At this voltage, the series current in the transmission line is proportionately large, being normally of the order of 1000 A. The corona current, on the other hand, is typically of the order of 10^{-3} A/meter. Thus, in one meter of line, the current loss is only about one part in a million. The extreme smallness of the attenuation amply justifies the neglect of the second-order partial derivative with respect to z in (121).

SECTION 6

CONCLUSIONS

This report comprises a study of the physics and the mathematics of the electrical corona on a long wire. The fundamental physical processes of collision ionization, ion drift and diffusion, which underlie much of the gas breakdown phenomena, were discussed at considerable length. They were transcribed into precise mathematical language in terms of a set of coupled nonlinear partial differential equations. A number of boundary-value problems for these basic equations were worked out. The calculations for the d-c and microwave breakdown fields, and for the d-c voltage-current characteristic, were found to be in good agreement with experiment. These successes provided solid support to the correctness of the basic equations.

With the exception of the transmission-line problem in Section 5, the boundary-value problems solved in this study are time-independent problems. This is not to suggest that the time-dependent problems are not of primary interest, but rather that they are by far harder to tackle. The mathematical equivalent of a transition from a time-independent corona phenomenon to a time-dependent one is a passage from nonlinear ordinary differential equations to nonlinear partial differential equations. The range of mathematical techniques available today for handling the latter type of equations is severely limited. And yet the study of many important aspects of the electrical corona will involve time-dependent problems.

In Subsection 5.2, the d-c corona voltage-current characteristic was applied to calculate the corona effect on pulse propagation along a transmission line. It is to be noted that although the problem is time-dependent, the treatment of the corona itself is quasi-static. This procedure is reasonable only if the shunt voltage at a fixed point on the line changes but little during the time it takes for the corona current to establish a steady flow. The latter time is at least as long as the transit time for an ion to travel from one conductor to another. An ion in air typically picks up a velocity of 1 cm./sec. in a field of 1 volt/cm. At breakdown, a representative ion velocity is about 1 km./sec. If the conductor separation is 1 meter, the transit time is about 10^{-3} second. One can surmise that if the width of a pulse, or the period of a continuous wave, is smaller than this value, the d-c result will be inapplicable.

A time-dependent treatment of the corona current must be considered.

Another problem in which time-dependence is essential is that of the corona effect on the trailing-wire antenna. During operation, the greater part of this antenna is hung in mid-air, far away from other conductors. There is no d-c equivalent of this configuration, since the d-c corona current always flows between two electrodes. The fact is that, under a continuous-wave excitation, the antenna is alternately anode and cathode. The ions in the corona oscillate in and out radially near the wire surface, more or less in phase with the wave. If there is a constant corona ohmic loss per cycle, then the power loss due to corona is directly proportional to the wave frequency, as was experimentally found by Peek in Eq. (3). At high frequencies, the loss is potentially very large. Obviously a theoretical attempt to deduce Peek's empirical result entails the solution of a time-dependent problem.

The analysis of the corona effect on aircraft antennas is a challenging theoretical problem. Its difficulty is enhanced by the scarcity of antenna data to guide the calculations. This preliminary study has been directed at identifying the basic physical processes and the basic mathematical problems involved. It has been concluded that Eqs. (9) through (13) are the basic irreducible equations for the corona phenomenon. Their essential correctness has been established by the good agreement between calculation and measurement in the quasi-static limit. The next stage in the overall corona effort will involve the study of time-dependent solutions of the basic equations. These will describe both the EMP and CW excitations of long-wire antennas. The chief quantities to come out of the calculations will be the corona charge and current densities around the antennas as a function of space and time, and of the sources of excitation. From these results one can analyze such corona effects as antenna signal distortion, power loss, and the corona modification of the coupling between aircraft and antennas.

REFERENCES

1. F.W. Peek, Jr., Dielectric Phenomena in High-Voltage Engineering, McGraw-Hill Book Company, New York, 1929.
2. J.D. Cobine, Gaseous Conductors, Dover Publications, New York, 1958.
3. J.D. Stephenson, "An experimental study of electrical discharge in gases at normal temperatures and pressures," Proceedings of the Physical Society (London) 45, 20-40 (1933).
4. A. von Engel, Ionized Gases, Oxford University Press, London, 1965, p.256.
5. J.S. Townsend, Electricity in Gases, Oxford University Press, New York, 1914.
6. J.D. Cobine, op. cit., p. 159.
7. F.W. Peek, Jr., op. cit. p. 61.
8. A.D. MacDonald, Microwave Breakdown in Gases, John Wiley and Sons, New York, 1966, Chap. 6.
9. M.A. Herlin and S.C. Brown, "Electrical breakdown of a gas between coaxial cylinders at microwave frequencies," Physical Review 74, 910-913 (1948).
10. J.S. Townsend, "Die Ionisation der Gase," Handbuch der Radiologie Band I, Akademischer Verlag, Leipzig, 1920, p. 332. See also J.D. Cobine, op. cit., pp. 258-261.
11. H. Albrecht, E. Wagner and W.H. Bloss, "Berechnung und Messung der Entladungscharakteristik einer positiven Korona," Elektrotechnische Zeitschrift 94, 599-603 (1973).
12. F. Borgnis, "Strömleitung durch Konvektion und Diffusion in zylindrischen Anordnungen," Annalen der Physik, 5. Folge, 31, 745-754 (1938).
13. I.B. Chekmarev, "Weakly charged gas between coaxial electrodes," Soviet Physics - Technical Physics 14, 1692-1695 (1970).
14. T.M. Ilinova and R.V. Khokhlov, "Wave processes in lines with nonlinear shunt resistance," Radio Engineering and Electronic Physics 8, 1864-1972 (1963).